GEOCHEMICAL, MINERALOGICAL, TEXTURAL AND MAP DATA FOR CRYSTAL-RICH, CALDERA FACIES HELLS MESA TUFF AND A COMAGMATIC LAVA DOME, CENTRAL NEW MEXICO: WITH A NOTE ON COMPOSITIONAL ZONING

Open-file Report 568

By
Richard M. Chamberlin

New Mexico Bureau of Geology and Mineral Resources
New Mexico Institute of Mining & Technology
Socorro, New Mexico 87801

January, 2015

Supersedes NMBG&MR Open-file Report 458

CONTENTS:

Introduction……………………………………………………………………………..4

Methods…………………………………………………………………………………6

Geologic Map Data……………………………………………………………………...8

Modal Mineralogy and Textural Data…………………………………………………..12

Whole-rock Geochemical Data…………………………………………………………13

Compositional Zoning…………………………………………………………………..17

References………………………………………………………………………………20

TABLES:

Table 1. Modal mineralogy and textural data for caldera-facies Hells Mesa Tuff and a comagmatic lava dome……………………………………………………………………..23

Table 2. Whole-rock geochemical data for caldera-facies Hells Mesa Tuff and a comagmatic lava dome……………………………………………………………………..24

Table 3. Modal mineralogy (volume %) and maximum crystal size (mm) from a measured section of the Hells Mesa Tuff outflow sheet near Magdalena (Brown,1972)…… 25

Table 4. Modal mineralogy (volume %) and maximum crystal size (mm) for the Hells Mesa eruptive sequence……………………………………………………………………26

Table 5. Whole-rock major element data available for the Hells Mesa magmatic suite (n =51)……………………………………………………………………………….....27

Table 6. Whole-rock trace element data available for the Hells Mesa magmatic suite (n =51)………………………………………………………………………………...28

Table 7. Whole-rock geochemical data for unaltered and slightly altered samples of the Hells Mesa magmatic suite (n=11)……………………………………………………....29

Table 8. Whole-rock geochemical data for post-Hells-Mesa rhyolite units (30.0-28.7 Ma) erupted from vent areas within and adjacent to the eastern Socorro caldera…………… 30

FIGURES:

Figure 1. Structural index map of the eastern Socorro caldera…………………………….31

Figure 2. Geologic map of the Bursum mine area……………………………….……32

Figure 3. Geologic map of the Torreon Springs area…………………………………….33

Figure 4. Geologic map of the Esperanza mine area…………………………………….34

Figure 5. Schematic stratigraphic section of Hells Mesa facies in the eastern Socorro caldera………………………………………………………………………………………35

Figure 6. Quartz content vs. relative stratigraphic position for the Hells Mesa eruptive sequence……………………………………………………………………...36

Figure 7. Maximum crystal size vs. crystallinity for Hells Mesa eruptive sequence……37

Figure 8. Ba vs. sanidine content for unaltered Hells Mesa rocks at the Esperanza Mine and a sanidine-granite clast in dome-derived tuff breccias………………………………38

Figure 9. SiO_2 vs. groundmass (melt) content in caldera-facies Hells Mesa rocks……...39

Figure 10. K_2O/Na_2O vs. Na_2O for K-metasomatized Hells Mesa rocks near the Bursum mine and unaltered Hells Mesa rocks near the Esperanza mine ………………………..40

Figure 11. Histogram showing SiO_2 variation in the Hells Mesa eruptive suite (n = 34). Normalized data from Table 5…………………………………………………….......41

Figure 12. Nb vs. Zr/TiO_2 for Oligocene rhyolites erupted from the eastern Socorro caldera at 31.9, 30.0, 28.8 and 28.7 Ma. Data from Tables 2 and 8……………………42

Figure 13. Total alkali--silica classification of unaltered Hells Mesa magmatic suite. Data from Table 7…………………………………………………………………….…43

Figure 14. Immobile element discrimination diagram (SiO_2 vs. Zr/TiO_2) for unaltered Hells Mesa magmatic suite. Data from Table 7…………..44

Figure 15. Immobile element discrimination diagram (Zr/TiO_2 vs. Nb/Y) for unaltered Hells Mesa magmatic suite. Data from Table 7…………………………………………45

INTRODUCTION

This report presents phenocrystic mineral modes, textural data, geochemical data and detailed geologic maps of caldera-facies Hells Mesa Tuff and a slightly younger comagmatic lava dome with dome-derived tuff breccias that are exposed in the eastern and southwestern sectors of the Socorro caldera (Fig1). This data was initially presented in support of an article entitled *Waning-stage Eruptions of the Oligocene Socorro Caldera, Central New Mexico,* which was published by the New Mexico Natural History Museum in their Bulletin 18, Volcanology in New Mexico (Chamberlin, 2001b). These data sets supplement a detailed report on the geology, hydrothermal alteration and mineralization within the Luis Lopez quadrangle (Chamberlin and Eggleston 1996), a revised geologic map of the Luis Lopez quadrangle (Chamberlin, Eggleston and McIntosh, 2002) and a $^{40}Ar/^{39}Ar$ geochronology study of the eastern sector of the Socorro caldera, source of the Hells Mesa Tuff (Chamberlin, McIntosh and Eggleston, 2004). This report supersedes NMBG&MR Open-file Report 458 (Chamberlin, 2001a); it includes several previously unpublished data tables and derivative data plots.

Three new data sets are presented: 1) detailed geologic maps of upper caldera-facies Hells Mesa Tuff and a comagmatic lava dome with derivative tuffs, showing maximum-clast-size distributon patterns of comagmatic-lithic lag breccias, inferred vent areas, and locations of 14 representative samples (Figs. 2-4); 2) modal mineralogical and textural analyses of 14 representative thin sections by the author using a Zeiss petrographic microscope and Swift automatic point counter (Table 1); and 3) X-ray fluorescence spectrometry analyses of 9 (of 14) whole-rock samples done by Chris McKee at the NMBG/NMT XRF lab to determine major oxide concentrations and abundance of 17 trace elements (Table2). These data sets allow comparison of modal mineralogy with geochemical trends in the upper caldera facies tuffs and the comagmatic lava dome. Three of the 14 samples were collected from a xenolith-poor zone near the top of the underlying lower caldera-facies Hell Mesa Tuff; again to allow comparison. Thin sectioned samples from the Torreon Springs area have not been chemically analyzed.

New data are compared to and integrated with published and unpublished data sets from previous investigations that represent: 1) the densely welded Hell Mesa outflow sheet near Magdalena (modal mineralogy from Brown, 1972); 2) hydrothermally altered and mineralized caldera-facies lower Hells Mesa Tuff (whole-rock geochemistry; Eggleston et al., 1983; Chamberlin and Eggleston, 1996); and 3) random samples of K-metasomatized Hells Mesa Tuff and recycled Hells Mesa clasts in younger metasomatized formations collected to study the chemistry and mineralogy of K-metasomatism in the Socorro region (whole-rock geochemistry; Ennis, 1996).

C.E. Chapin graciously provided archived thin sections from Brown's measured section of the outflow sheet (Brown, 1972) so the author could make measurements of maximum crystal sizes in the densely welded tuffs. Maximum-crystal-size data, Brown's original modal data, and the stratigraphic position of samples are all listed in Table 3. Data from Table 3 are combined with modal data from this study (Table 1) in order to examine mineralogical trends for the entire Hells Mesa sequence (Table 4) with respect to their relative stratigraphic position. Available and complete whole-rock geochemical analyses (i.e. include LOI data) for the Hells Mesa eruptive suite are listed in Tables 5 and 6 (n=51). Seventeen of these available analyses apparently represent moderately to intensely altered rocks, mineralized rocks, or inaccurate analyses; the latter are indicated by statistical outlier values or high totals. The remaining 34 analyses, which include 23 K-metasomatized samples, are used to calculate mean SiO_2 content of the Hells Mesa eruptive suite, since the SiO_2 content of tuffs is not significantly affected by K-metasomatism

(Dunbar et. al., 1994). Analyses of 11 unaltered to slightly altered Hells Mesa rocks are listed in Table 7; mean values of these samples are considered to be the most representative of the Hells Mesa magmatic suite (not considering volatile elements). Finally, new geochemical data for the upper Hells Mesa tuffs and comagmatic lava dome are compared to geochemical data from post Hells Mesa rhyolite units erupted from the eastern Socorro caldera (Table 8; Chamberlin et. al., 2004); this allows an examination of upper-crustal magmatic evolution over a span of 3.2 million years (31.9-28.7 Ma). Note that all $^{40}Ar/^{39}Ar$ age determinations presented here are based on an accepted age of 27.84 Ma for the Fish Canyon sanidine monitor.

METHODS

Geologic mapping of the upper-caldera facies Hells Mesa Tuff, and tuff breccias derived from a comagmatic lava dome (Figs. 1-4), emphasized field measurements of the maximum size of comagmatic clasts within outcrops of the crudely bedded coignimbrite lag breccias, which may also be referred to as autolithic ignimbrites. Mapping traverses were made primarily along strike to observe lateral variations in one or more depositional units at about the same stratigraphic level. Secondary traverses were made roughly perpendicular to strike at spacing of about 100-200 m, as outcrop patterns permitted or dictated. Clast sizes were measured with a 33 cm-long rock hammer graduated at 5cm and 1cm increments. Field measurements of larger clasts (>50 cm) are considered to be accurate to ± 5 cm and smaller clasts to ± 1-2 cm.

Petrographic analyses of thin sections (Table 2) were completed using a Zeiss petrographic microscope. Maximum phenocryst sizes were measured with the petrographic microscope using a graduated eyepiece (one division = 0.038 mm at a magnification of 31.25 x). Thin sections were scanned with a hand lens to locate the largest crystal, which was then measured to the nearest 0.1 mm (± 0.1 mm). Modal mineral analyses were made using a Swift automatic point counter set at an interval spacing of 1mm by 1mm, which is approximately equal to the mean phenocryst size for most of these crystal-rich rocks. Mineral species were identified using optical properties as catalogued by Kerr (1959) and by Deer, Howie and Zussman (1966). In unaltered rocks, untwinned sanidine crystals could only be confidently discriminated from quartz by obtaining interference figures (as point counts progressed). In K-metasomatized samples from the Bursum mine area , plagioclase phenocrysts are completely replaced by delicate lattice-works of adluaria and clay minerals that commonly wash out of the thin section during preparation. Euhedral holes with bits of clay along the edges are counted as phenocrystic plagioclase in these altered rocks; likewise rhombic outlines associated with leucoxene are counted as sphene crystals.

Three repeated analyses of one sample (Table 2, E1) indicate that counting errors decrease with increasing abundance of a mineral phase. Total phenocryst contents are estimated to be reproducible to about ± 2 vol. % at a total of 40 vol. % crystals. Counting errors for phenocrystic quartz are estimated at ± 10% at a total quartz content of 10% (i.e. modal quartz = 10 ± 1 vol. %). Measurement errors for minor phases such as biotite and magnetite/hematite are as high as ± 50%. Coarse-grained samples (phenocrysts > 5 mm) yield more erratic volumetric estimates of modal mineralogy because of the "nugget" effect, which is exacerbated by a small sample size (standard thin section ~ 22 x 40 mm). Total crystal contents for coarse-grained rocks are probably reproducible at about ± 5 vol. %.

Four samples from the Bursum mine area and five samples from the Esperanza mine area were submitted for whole-rock geochemical analyses at the NMBG XRF lab. Analytical methods are described in the footnote to Table 2. Repeat analyses at the NMBG XRF lab (n=148) indicate wt% SiO_2 concentrations are reproducible to ± 1.1 wt.% at a total silica content of 71.35 wt %

(95% confidence, $\pm 2\sigma$). Other oxide concentrations are precise to about ± 2-3%, except for P_2O_5 (± 10%). Trace element analyses are reproducible to ± 10-25 %, except for As, V, Mo and Cr, which have associated analytical errors of ± 35-70% (as the method approaches detection limits for these elements).

GEOLOGIC MAP DATA

Crystal-rich, caldera-facies Hells Mesa Tuff is divided into lower and upper members on the basis of the lithology of entrained lithic fragments (Chamberlin and Eggleston, 1996; Chamberlin et al. 2002; Fig 1). The lower caldera-facies Hells Mesa contains a variety of older Tertiary volcanic fragments (mostly andesites) and clasts of pre-Tertiary rocks such as limestone, sandstone, schist and granitic rocks. Fragments of older country rock that occur in the densely welded tuffs are referred to as *xenoliths*. The basal caldera-facies tuffs are xenolith rich and contain large blocks of older country rock interpreted as landslide megabreccias derived from contemporaneous collapse of an oversteepened caldera wall (along the south margin). The top of the lower caldera-facies Hells Mesa Tuff is xenolith-poor. In general, the lower caldera-facies Hells Mesa Tuff can be referred to as xenolithic, or xenolith bearing. Near Torreon Springs the top 20m of the lower xenolithic member is moderately to poorly welded and forms a recessive valley or swale between the lower and upper members. Stratigraphic relationships of caldera-facies Hells Mesa Tuff (in the eastern sector of the caldera) and a slightly younger ring-fracture lava dome and derivative tuff breccias are schematically illustrated in Figure 5. Local facies of the upper Hells Mesa Tuff near Torreon Springs (Thu) occupy the same stratigraphic position as the bedded tuff zone (Thuf, Fig. 5) at the Bursum mine.

The upper caldera-facies Hells Mesa Tuff tends to be crudely bedded and contains abundant to rare fragments of red crystal-rich rhyolite compositionally similar or identical to the enclosing crystal-rich tuffs. These red rhyolite clasts are referred to here as comagmatic lithics (synonymous with autoliths). Field relationships and textural characteristics support their interpretation as coignimbrite lithic lag breccias (clasts of normal-rock density) carried only a few kilometers from their source vent (Wright and Walker, 1977).

Near the Bursum mine (Fig.2), the depositional contact between the upper and lower members of the caldera-facies Hells Mesa Tuff (Thu/Thx) is gradational and densely welded. This subtle contact is marked by the upward disappearance of rare small andesitic xenoliths and appearance of rare small clasts of red spherulitic rhyolite near the base of a 200m thick massive zone (Thu, Fig.5). A thin fine-grained ash-fall bed occurs about 10 meters above this subtle gradational contact between lower and upper Hells Mesa Tuff. A poorly welded recessive zone about 20m thick locally occurs at the top of the massive lower zone (Thu). Above this cooling break, a distinctly bedded zone (Thuf, Fig.5) approximately 200m thick, contains numerous fall deposits and coarse comagmatic lag breccias. About 15-20 ledge-forming depositional units are visible in the field, and on aerial photographs of the upper bedded zone, where well exposed about 1 km ESE of the Bursum mine.

A 2-cm-thick "sandy" winnowed layer (~ 90% fine- to medium-grained crystals) occurs immediately above an ash-rich fall deposit near the base of the bedded zone (outcrop location shown on Fig.2). This rare lithology extends a few tens of meters along strike. It may represent a "volatile-jet" driven separation of heavier crystals from finer-grained ash at the toe of an advancing pyroclastic flow, or some other type of high-velocity wind deposit such as a material left behind a “volcanogenic tornado”.

Detailed geologic maps of the Bursum mine, Torreon Springs and Esperanza mine areas are shown as Figs. 2-4. Mapping concentrated on determining maximum clast size distribution patterns in the crudely bedded ignimbrites and comagmatic lag breccias. Field observations of clast textures and clast geometries (commonly angular to equant) indicate that most of them were emplaced at normal rock densities and do not represent compacted pumice. However, some moderately flattened spherulitic clasts in the Bursum mine area apparently represent "soft" slightly compressible microcrystalline mush at the time of emplacement. The maximum clast size observed in a typical continuous outcrop (e.g. ~10 -20 m long) is commonly about twice the size of the most abundant megascopic clasts. Distribution patterns of maximum clast size are used to estimate the general transport direction of the lag breccia deposits and the approximate distance from the coarsest outcrops to the inferred vent area (Figs. 1-4).

The "downstream" distance, through which the maximum clast size decreases by a factor of two, can be used as a rough indicator of the average transport energy associated with a particular vent area. This "transport-energy factor" is about 1300-1400 m for the lag breccias near Torreon Springs, about 500-600 m for the Bursum mine facies and 400-500 m for the Esperanza mine facies. Post-depositional rift faulting has clearly distorted (stretched) the maximum-clast-size isopleths near the Bursum mine (Fig. 2). Vent areas (Fig. 1) are inferred where extrapolated clast sizes approach 3-6 m in the "upstream" direction.

Lag breccias near the Bursum mine are characterized by clasts of phenocryst-rich rhyolite that exhibit spherulitic crystallization of the red groundmass. Lag breccias in the Torreon Springs area are formed by angular fragments of densely welded lower Hells Mesa Tuff that occasionally contain smaller xenoliths of dark gray andesite within the younger generation of explosively fragmented (recycled) ignimbrite. Blocky tuff breccias near the Esperanza mine (Trt) are lithologically equivalent to the crest of the small lava dome exposed about 1 km to the south;

these northward fining breccias were apparently erupted from a vent near the north flank of the dome (Fig. 4).

The comagmatic lag breccias are apparently derived from different vent areas and display different stratigraphic patterns with respect to clast size distribution . The Bursum mine facies (Thu & Thuf) coarsens upwards through as much as 400 m of mostly densely welded tuffs. Breccia clasts as much as 75 cm long occur near the top of the Bursum mine sequence. The Torreon Springs facies (Thu) appears to be coarsest near the middle of the 200m thick unit. Complete sections of moderately welded tuffs, which are exposed in fault blocks west of Torreon Springs (Fig.3), coarsen upwards toward the medial zone and then fine upwards toward the top of the map unit. The lower, medial and upper breccia zones near Torreon Springs generally become finer grained to the south-southwest, although the pattern is more erratic than at the Bursum mine or the Esperanza mine. The poorly to moderately welded dome-derived tuffs north of the Esperanza mine (Trt) are coarsest near the base of the 60-120m thick sequence. This basal blocky breccia unit coarsens uniformly toward the south and the exposed crest of the coeval lava dome (Fig. 4).

Approximately 30-40 m of mostly densely welded "Thu" equivalent conformably underlie the blocky tuff breccias (Trt) north of the Esperanza mine (Chamberlin et al., 2002; Fig.5). Red rhyolitic clasts in this thin zone are small (2-10cm) and sparse (1-3%). Small andesitic lithics also occur rarely, which locally makes this thin zone difficult to distinguish from the underlying xenolith-poor, lower Hells Mesa Tuff (Thx). About 0.7 km north of the Esperanza mine, the uppermost 7m of Thu is a friable poorly welded or non-welded zone; this welding break suggests a hiatus of perhaps 10^3 -10^4 years between upper Hells Mesa pyroclastic eruptions and emplacement of the coarsely porphyritic lava dome.

Inferred vent areas for the upper lag-breccia facies and the comagmatic lava dome roughly define an inner ring fracture zone about 7 km in diameter (Fig.1). The elliptical shape shown on Fig. 1 reflects post-caldera stretching (crustal extension) to the WSW, which is associated with the Rio Grande rift.

MODAL MINERALOGY AND TEXTURAL DATA

Modal mineralogy and textural data for 14 thin sections of caldera-facies Hells Mesa Tuff and a comagmatic lava dome with associated tuffs are summarized in Table 1. The Hells Mesa Tuff exhibits a phenocrystic mineral suite characteristic of a metaluminous arc-related rhyolite. In order of decreasing overall abundance, the major mineral phases are sanidine, plagioclase and quartz with minor biotite and opaques (magnetite/hematite). Trace amounts of sphene, apatite and zircon are typical of most samples from the Hells Mesa. A few reflected light observations and mass-balance comparison of geochemical data (i.e. TiO_2 and TiO_2/Fe_2O_3) with modal mineralogy (Tables 1 and 2) suggest that ilmenite is not present as a significant component of the opaques.

Samples were collected in order to represent each major lithology observed in the upper caldera- facies tuffs and the dome-derived tuff breccias. These lithologies include: crystal-rich tuff, crystal-rich comagmatic breccia clasts, and the lava dome itself. Rare clasts of granite observed in the Torreon Springs and Esperanza mine facies tuffs were also collected to evaluate their origin.

Samples E1 and E2 both represent the comagmatic lava dome, although the latter is from a 3.1m block of flow-banded rhyolite within the dome derived tuffs (Fig.4). Field relationships, identical mineral suites, and equivalent textures (such as compositionally zoned sanidine crystals) all indicate these samples are from the same eruptive unit. However, the dome sample contains significantly less crystals (45%) versus the lava block, which contains ~59 % crystals. The average of these two analyses, 52 vol. %, is considered to be the best estimate for the total crystal content of the lava dome. The large variation in measured crystal content is attributed to non-uniform melt distribution in the granular mush (possibly related to dilation along shears; e.g. Smith, 1997) and the "nugget" effect of coarse phenocrysts of sanidine and quartz that occur in the relatively small samples (standard thin sections, 22 x 40 mm).

Upper Hells Mesa Tuffs and the slightly younger comagmatic lava dome are all quartz rich and crystal rich. A plot of quartz content versus relative stratigraphic position shows that the top of outflow facies at Magdalena is compositionally similar to the top of the lower caldera-facies Hells Mesa Tuff (Fig.6). The maximum size of phenocrysts in the Hells Mesa outflow and caldera-facies units shows a general positive correlation with crystallinity, or total phenocryst content (Fig. 7).

Taken together, figures 6 and 7 illustrate that the lower Hells Mesa outflow sheet and the post-collapse lava dome both approached a crystallinity flow barrier at about 55% total crystals. Just prior to eruption, about half of the Hells Mesa magma body must have been a rigid mush of interlocking crystals and interstitial melt at the cooler margins of the body (cf. Marsh, 1989). Some dynamic event, such as collapse of the magma chamber roof, presumably disrupted the peripheral rigid mush in order to allow continued ash-flow eruptions that formed the upper half of the outflow sheet (Fig.6).

Coarse-grained granite clasts in the tuff breccias near the Esperanza mine are mineralogically similar to the Hells Mesa Tuff (Table 1; E4 & E5). However, these sanidine granites lack compositionally zoned sanidine phenocrysts typical of the Hells Mesa-age lava dome (31.89 ± 0.16 Ma; Chamberlin et al., 2004) and the dome-derived tuffs (Table 1). Chemical data, discussed in the following section (Fig.8), indicate the sanidine-granite clasts are not comagmatic with the Hells Mesa Tuff, even though they are mineralogically similar. Rare granite clasts near Torreon Springs (Table 1, T3; Fig. 3) contain abundant microcline and traces of monazite; they are clearly derived from Proterozoic basement rocks.

WHOLE-ROCK GEOCHEMICAL DATA

Whole-rock geochemical data for 9 samples collected from caldera-facies Hells Mesa rocks are listed in Table 2. Two of these samples are from the xenolith-bearing lower Hells Mesa Tuff (Thx) and seven are from the stratigraphically higher upper Hells Mesa (Thu and Thuf) and the stratigraphically youngest lava-dome related rocks (Trt and Tre, Fig. 5). One sample of sanidine granite was analyzed; it was collected from the basal blocky zone of the dome-derived tuffs north of the Esperanza mine (Fig 4, E4). Additional whole-rock geochemical data available for the Hells Mesa Tuff are listed in Tables 5 and 6.

A plot of Ba concentration (ppm) vs. sanidine content (vol. %) demonstrates a strong correlation ($r^2 = 0.99$) for different stratigraphic levels of caldera-facies Hells Mesa rocks (Fig.8). This plot also clearly shows that the sanidine-granite clast (E4, Table 2) is not comagmatic with Hells Mesa rocks at the Esperanza mine area. This unusual lithology — high-temperature alkali feldspar in a coarse-grained "low temperature" plutonic rock — is interpreted as a partially melted (contact metamorphosed) pendant of Proterozoic granite that was derived from the walls of the Hells Mesa magma chamber prior to eruption of the dome-related tuffs. Mylonitic shear bands and cataclastic textures in clasts of sanidine granite from the same locality suggest high temperature shearing and possibly explosive deformation of the granitic pendants during eruption of the dome-derived tuffs. Sanidine-granite clasts are about twice the size of adjacent lava blocks in the tuff-breccia outcrop ~1 km north of the lava dome (Fig.4). This size difference suggests that these unusual sanidine-granite clasts were carried rapidly upward from considerable depth by the pyroclastic eruption column and followed a different (higher) trajectory during emplacement. Rapid transport of these partially melted pendants of granite from the magmatic temperature environment to the surface caused quenching and preservation of the high-temperature sanidine.

Petrographic data and field relationships indicate that samples E1 and E2 are from the same lava dome, although the latter is from a large block in the dome-derived tuff breccia. At first glance, geochemical data, particularly SiO_2 content (Table 2), suggest that they are not genetically equivalent rocks. Slightly higher Fe_2O_3, TiO_2, V, Y, and Zr contents in E2 are readily explained by a higher content of opaques and slightly more sphene (Table 1). Sample E2 also contains minor calcite (~2%, note relatively high CaO content), which partially replaces plagioclase. Thus the SiO_2 content in this sample is slightly depressed (~ 1%) by the presence of secondary calcite. The ~ 5% difference in normalized SiO_2 content ($nSiO_2$, Table 2) is almost certainly real; this relationship suggests that the groundmass of the lava is a high-silica rhyolite (~77.5 % SiO_2) and that the feldspar-rich sample (E2) essentially forms a diluted melt (feldspars average about 65% SiO_2, Deer, Howie and Zussman, 1966). As shown in Figure 9, normalized SiO_2 shows a moderate positive correlation with total melt content ($r^2 = 0.69$) for the waning-stage Hells Mesa rocks and the uppermost lower Hells Mesa Tuff, which supports the above suggestion.

Samples from the Bursum mine area (B1-B4) are potassium metasomatized. Potassium metasomatism is best verified in thin section (Chamberlin and Eggleston, 1996), but it is also typically indicated by K_2O/Na_2O ratios above 3 to 3.5, and commonly by Na_2O concentrations less than 2.0 wt % (Fig10). Soda, potash, Rb, Sr, Ba and other mobile elements have been redistributed by metasomatism in the Bursum mine area and are not representative of compositional trends in the Hells Mesa magma chamber.

Thirty four analyses of relatively unaltered and K-metasomatized rock samples from the Hells Mesa eruptive suite (Tables 5 and 6, unshaded sample numbers) yield a mean normalized silica content of 73.4 ± 1.5 wt. % SiO_2. A histogram of silica content for the Hells Mesa suite shows that most samples range from 69-75 % SiO_2 (Fig. 11) . The silica content of a rhyolite ignimbrite is generally unaffected by K-metasomatism (Dunbar, et.al., 1994).

The magmatic evolution of 4 rhyolitic eruptive centers in the eastern Socorro caldera, from 31.9 to 28.7 Ma, is illustrated by a plot of Zr/TiO2 vs. Nb as shown in Fig. 12. From youngest to oldest the eruptive units are: La Jencia Tuff, upper rhyolite member of Luis Lopez Formation, medial tuff Member of Luis Lopez Formation, and Hells Mesa Tuff: dated respectively at 28.7, 28.8, 30.0 and 31.9 Ma (Chamberlin et. al., 2004). The diagram illustrates a general decrease in Nb content with time for the older two units, and a later increase in Zr/TiO2 ratio with time. The origin of these magmatic trends is unknown.

Unaltered samples of the Hells Mesa magmatic suite (Table 7) are plotted on a total alkali --silica classification diagram (Fig. 13). Their classification as rhyolites is consistent with the observation of abundant phenocrystic quartz and sanidine in hand specimens (Chamberlin and Eggleston, 1996). It is inappropriate to plot K-metasomatized and hydrothermally altered samples on a total alkali--silica diagram.

Immobile element discrimination diagrams have been used to classify the magmatic series of hydrothermally altered samples (Winchester and Floyd, 1977). Immobile element plots for unaltered rocks of the Hells Mesa suite (Table 7) are shown as Figs. 14 and 15. The plot of

SiO_2 vs Zr/TiO_2 (Fig. 14) classifies the Hells Mesa suite as transitional between rhyolites and dacites. The Zr/TiO_2 vs. Nb/Y plot (Fig. 15) indicates a "trachyandesite" composition for these silica-rich rocks. Zr/TiO_2 can be a proxy for silica content and Nb/Y is proxy for alkalinity (i.e., total alkalis). The relatively low Zr content and slightly elevated Y content of the Hells Mesa magma suite has "pushed" it into the trachyandesite domain; perhaps this reflects a "parental" andesitic arc-related magma that evolved into the rhyolitic Hells Mesa suite.

COMPOSITIONAL ZONING

Many large volume caldera-forming ignimbrites exhibit compositionally zoned outflow sheets (Lipman et al., 1966; Hildreth, 1981). Large volume, densely welded ignimbrite sheets, such as the Hells Mesa Tuff (1200 km^3, McIntosh et al., 1991), must be erupted in a few days to weeks. Most compositionally zoned ignimbrite sheets exhibit a progressive upward increase in crystal content and general decrease in bulk silica content. Zoned ignimbrites with a basal zone of crystal-poor high-silica rhyolite and an upper zone of crystal-rich dacite are commonly interpreted as the product of large zoned magma chambers that were rapidly emptied from the top down (Lipman, 1967; Smith, 1979; Wolff et al., 1990). The high-viscosity of silicic magmas precludes crystal settling as a mechanism to produce crystal-rich zones in the lower part of ignimbrite magmas (Glazner, 2014). Many large-volume crystal-rich ignimbrites, such as the Fish Canyon Tuff of Colorado, are relatively homogeneous and lack vertically zoned outflow sheets (Lipman, 2000; Bachmann and Bergantz, 2008)).

The Hells Mesa Tuff is crystal-rich throughout (30-55% crystals, Table 4) and is compositionally zoned with respect to phenocrystic quartz content. The lower 1/3 of the outflow sheet in the southern Bear Mountains north of Magdalena (Brown, 1972) exhibits a progressive and nearly linear upward increase in phenocrystic quartz (~1 to 11 vol.%) and total crystals

(Samples M1-M8, Table 3, Fig.6). About 250 feet above the base, the trend of increasing quartz and crystal content is disrupted and becomes jumbled within the middle of the sheet (Fig.6). However the uppermost outflow and the uppermost caldera-facies continue the initial trend of upward increasing crystal content (45-50%) and quartz content (14-15 %). Osburn and Chapin, 1983a (p. 200) interpreted the caldera-facies Hells Mesa Tuff exposed in the northern Magdalena Mountains as “reversely zoned” from a quartz-poor intermediate basal zone to a felsic quartz-rich upper interval. Available geochemical data (Table 5, Fig.11) shows the Hells Mesa Tuff ranges from 69-76 % SiO_2 with mean composition of about 74 % SiO_2; unfortunately geochemical data with respect to stratigraphic position is mostly lacking. With respect to total crystal content, the Hells Mesa Tuff is similar to most zoned ignimbrites that show an upward increase in crystal content. More work is needed to determine the vertical zonation of bulk silica content in the Hells Mesa Tuff.

The apparently robust zonation of phenocrystic quartz in the Hells Mesa Tuff and accompanying upward increase in crystal abundance and size suggests that prior to eruption, the cooler outer margins of the large magma body consisted of a rigid mush of interlocking crystals (~55%) and interstitial melt (~45%) and the inner core of the magma body (~ ½ of total volume) consisted of a mobile crystal mush with 30-40% crystals (Marsh, 1989). If so, the magma chamber was initially tapped near its center and then emptied from the center outwards, as well as from the top down. Collapse of the magma chamber roof may have disrupted the peripheral rigid mush in order to allow continued ash-flow eruptions that formed the upper half of the outflow sheet (Fig. 6 and 7).

Several studies have shown that large volume silicic magmatic systems that produce caldera-forming eruptions are open systems, periodically recharged from below by more primitive magmas (Lipman, 2007; Charlier et al., 2007; Hildreth and Wilson, 2007; Bachmann and Bergantz, 2008). In the Joyita Hills, about 14 km northeast of the Socorro caldera (Fig.1), the Hells Mesa Tuff overlies about 20 m of locally erupted alkali-olivine basalt lavas (Tlp_1 of DeMoor et al., 2005), which represent the stratigraphically oldest member of the La Jara Peak Basaltic Andesite in the Socorro-Magdalena region (Osburn and Chapin, 1983b). Thus a permissible, but not required, interpretation could be that the largely crystalline Hells Mesa magma system was "goosed" and reactivated by a La Jara Peak type basalt intrusion into the base of the mushy magma body shortly before the caldera-forming eruption. The large volume (7000 km^3) Socorro-Magdalena caldera cluster of Oligocene age (32-24 Ma) was apparently fueled by lower crustal sill-like intrusions of La Jara Peak type basaltic andesites, which also leaked out the margins of the large long-lived magma system (Chapin et al, 2004; Chamberlin et al., 2012). The thermal zonation of the Hells Mesa magma body prior to eruption could presumably be ascertained by a "Ti-in-Quartz" thermometry study similar to that done by Wark et al ., 2007.

REFERENCES:

Bachmann, O. and Bergantz, G.W., 2008, Deciphering Magma Chamber dynamics from Styles of Compositional Zoning in Large Silicic ash Flow Sheets: Reviews in Mineralogy & Geochemistry, Vol. 69 p. 651-674.

Brown, D. M., 1972, Geology of the southern Bear Mountains, Socorro County, New Mexico: M.S. Thesis, New Mexico Institute of Mining and Technology, 110 p. New Mexico Bureau of Mines and Mineral Resources, Open-file Report 42, 110 p.

Chamberlin, R.M., 2001a, Modal mineralogy, textural data and geochemical data for caldera-facies Hells Mesa Tuff and a comagmatic lava dome, with selected data plots and supporting map data: New Mexico Bureau of Geology and Mineral Resources Open-File Report 458, 39p.

Chamberlin, R.M., 2001b, Waning-stage Eruptions of the Oligocene Socorro Caldera, Central New Mexico, *in* Volcanology in New Mexico, L.S. Crumpler and S.G. Lucas (eds.), New Mexico Museum of Natural History and Science Bulletin 18, p. 69-77.

Chamberlin, R. M. and Eggleston, T. L., 1996, Geologic map of the Luis Lopez 7.5 minute quadrangle, Socorro County, New Mexico: New Mexico Bureau of Mines and Mineral Resources Open-file Report 421, 147 p.

Chamberlin, R.M., Eggleston, T.L., and McIntosh, W.C., 2002, Geologic map of the Luis Lopez quadrangle, Socorro County, New Mexico: New Mexico Bureau of Geology and Mineral Resources Open-file Geologic Map, OFGM-53.

Chamberlin, R.M., McIntosh, W.C. and Eggleston, T L., 2004, $^{40}Ar/^{39}Ar$ Geochronology and Eruptive History of the Eastern Sector of the Oligocene Socorro Caldera, Central Rio Grande Rift, New Mexico: *in* Tectonics, Geochronology and Volcanism in the Southern Rocky Mountains and Rio Grande Rift; S.M. Cather, W. C. McIntosh, and S.A. Kelly (eds.): New Mexico Bureau of Geology and Mineral Resources Bulletin 160

Chamberlin, R.M., McIntosh, W.C., Dunbar, N.W., and Dimeo, M.I., 2012, Ignimbrite calderas and a large radiating mafic dike swarm of Oligocene age, Rio Grande rift, New Mexico: Possible implications to restless calderas (abs.): Volcanism in the American Southwest: http://volcanoes.usgs.gov/vsc/file_mngr/file-62/VASW_Abstract_Volume.pdf

Chapin, C.E., McIntosh, W.C., and Chamberlin, R.M., 2004, The Late Eocene-Oligocene Peak of Cenozoic Volcanism in Southwestern New Mexico: *in* The Geology of New Mexico: A Geologic History (G.H. Mack, K.A Giles and G.S. Austin eds.), New Mexico.

Charlier, B.L.A., Bachmann O, Davidson JP, Dungan MA, Morgan D., 2007, The upper crustal evolution of a large silicic magma body: evidence from crystal-scale Rb/Sr isotopic heterogeneities in the Fish Canyon magmatic system, Colorado. J Petrol 48:1875-1894

Cox, K.G., Bell, J.D., and Pankhurst, R.J., 1979, The interpretation of Igneous Rocks: London: Allen and Unwin, 450 p.Geological Society Special Publication 11, p.271-293.

Deer, W. A., Howie, R. A., and Zussman, J., 1966, An introduction to the rock-forming minerals: Wiley and Sons, New York, N. Y., 528 p

DeMoor, M., Zinsser, A., Karlstrom, K., Chamberlin. R.M., Connell, S.D., and Read, A., 2005, Preliminary Geologic Map of the La Joya 7.5 minute Quadrangle: New Mexico Bureau of Geology and Mineral Resources Open-File Geologic Map, OFGM- 102.

Dunbar, N.W., Chapin, C.E., Ennis, D.J. and Campbell, A.R., 1994, Trace element and mineralogical alteration associated with moderate and advanced degrees of K-metasomatism in a rift basin at Socorro, New Mexico: New Mexico Geological Society Guidebook 45, p. 225-231.

Eggleston, T.L., Norman, D.I., Chapin, C.E. and Savin, S., 1983. Geology, Alteration and genesis of the Luis Lopez manganese district, New Mexico: New Mexico Geological Society Guidebook 34, p. 241-246.

Ennis, D.J., 1996, The effects of K-metasomatism on the mineralogy and geochemistry of silicic ignimbrites near Socorro, New Mexico: M.S.thesis, New Mexico Institute of Mining and Technology, Socorro, New Mexico, 160 p.

Glazner, A.F., 2014, Magmatic life at low Reynolds number: Geology, v.42, no.11, p.035-938.

Hildreth, W. S., 1981, Gradients in silicic magma chambers: Implications for lithospheric magmatism. J. Geophysical Research: v86, p. 10153-10192.

Hildreth, W.S., and Wilson C.J.N., 2007, Compositional zoning in the Bishop Tuff. J Petrol 48:951-999

Kerr, P. F., 1959, Optical Mineralogy, McGraw Hill, New York, 442 p.

Lipman, P.W., 2000, The central San Juan caldera cluster: Regional volcanic framework. In: Ancient Lake Creede: Its Volcano-Tectonic Setting, History of Sedimentation, and Relation of Mineralization in the Creede Mining District. Bethke PM, Hay RL (eds) Geol Soc Am Spec Paper 346:9-69.

Lipman, P.W. 2007, Incremental assembly and prolonged consolidation of Cordilleran magma chambers: Evidence from the Southern Rocky Mountain volcanic field. Geosphere 3:1-29

Lipman, P.W. 1967, Mineral and chemical variations within an ash-flow sheet from Aso caldera, South Western Japan. Contrib Mineral Petrol. 16:300-327

Lipman, P.W., Christiansen, R.L., and O'Connor, J.T., 1966, A compositionally zoned ash-flow sheet in southern Nevada: U.S. Geological Survey, Professional Paper 524-F, 47p

Marsh, B.D., 1981, On the crystallinity, probability of occurrence, and rheology of lava and magma: Contributions to Mineralogy and petrology, v.78, p.85-98.

Marsh, B.D., 1989, Magma chambers. Annu Rev Earth Planet Sci 17:439-474

McIntosh, W.C., Kedzie, L.L., and Sutter, J.F., 1991, Paleomagnetism and $^{40}Ar/^{39}Ar$ ages of ignimbrites, Mogollon-Datil volcanic field, southwestern New Mexico: New Mexico Bureau of Mines and Mineral Resources Bulletin 135, 79p.

Norrish, K. and Chappell, B. W., 1977, An accurate X-ray fluorescence spectrographic method for the analysis of a wide range of geologic samples: Geochimica Cosmochimica Acta, v. 33, p. 67-76.

Norris, K. and Hutton, J. T., 1969, X-ray fluorescence spectrometry, *in Physical Methods in Determinative Mineralogy,* ed. Zussman, Academic Press.

Osburn, G.R., and Chapin, C.E., 1983a, Ash-flow tuffs and cauldrons in the northeast Mogollon-Datil field: A summary:, New Mexico Geological Society Guidebook 34. p. 197-204.

Osburn, G.R., and Chapin, C.E., 1983b, Nomenclature for Cenozoic rocks of northeast Mogollon-Datil volcanic field, New Mexico: New Mexico Bureau of Mines and Mineral Resources Stratigraphic Chart 1, 7p. and 1 sheet.

Smith, R.L., 1979, Ash-flow magmatism. Geol Soc Am Spec Paper 180:5-25

Spradlin, E. J., 1972, Stratigraphy of Tertiary Volcanic Rocks, Joyita Hills Area, Socorro County, New Mexico: unpub. M. S. Thesis, University of New Mexico, 73p.

Wark, D.A, Hildreth, W.S., Spear, F.S., Cherniak, D.J., Watson, E.B., 2007, Pre-eruption recharge in the Bishop Tuff magma chamber. Geology 35:235-238

Winchester, J.A. and Floyd, P.A., 1977, Geochemical discrimination of different magma series and their differentiation products using immobile elements: Chemical Geology, v.20, p.325-343.

Wolff J.A., Worner, G., Blake, S., 1990, Gradients in physical parameters in zoned felsic magma bodies: implications for evolution and eruptive withdrawal: J Volcanol Geotherm Res 43:37-55

Wright, J.V., and Walker, G.P.L., 1977, The ignimbrite source problem, significance of a co-ignimbrite lag-fall deposit: Geology, v. 5, p. 729-73

Table 1. Modal mineralogy and textural data for caldera-facies Hells Mesa Tuff and a comagamatic lava dome.
Phenocrystic mineral data in volume %; tuffs recalculated as lithic free. Maximum crystal size in mm. Sample prefix indicates localitiy (Fig. 1):
E is Esperanza mine, T is Torreon Springs, B is Bursum mine. Sample locations shown on Figs. 2-4. Point counts made on 1x1 mm grid. K-metasomatized samples shown in bold.

Sample	Rock type	Field number	Quartz	Sanidine	Plagioclase	Biotite	Sphene	Magnetite [a]	Groundmass	Total	Counts	Lithics (clasts)	Total Crystals	Quartz/Feldspar	Max. Crystal Size	Textures
Comagmatic lava dome (Tre) and dome-derived tuff breccias (Trt): (tuff breccias contain lava clasts)																
E1 [b]	lava	LLZ-00-2	9.4	20.9	13.0	1.6	0.1	0.4	54.5	99.9	1342 [c]	0	45.4	0.28	6.9	mcg,sp,pks,mfx, ozs, eq
E2	lava clast	LLZ-00-4	10.1	28.5	17.0 [d]	1.7	0.2	1.2	41.3	100.0	424	100 [e]	58.7	0.22	8.2	sp,mcg-fb,pks,mfx,ozs,eq
E3	tuff	LLZ-00-5	16.5	25.4	12.3	2.5	tr [f]	1.2	42	99.9	405	0.8	57.9	0.44	5.8	cc,mcg,psp,pc,pks,ozs,eq
Upper caldera-facies Hells Mesa Tuff (Thu & Thuf): (contains comagmatic-lithic lag-breccia clasts)																
T1	tuff	TS-2	14.7	16.6	14.2	0.8	tr	1.3	52.3	99.9	382	2.4	47.6	0.48	3.7	cc,pc,psp,eq
T2	clast of tuff	TS-2A	12.7	19.5	15.5	1.5	0.2	0.8	47.9	99.9	394	100(3.4) [g]	50.2	0.36	4.5	cc,pc,psp,eu,ozs, eq
B1	**tuff**	**LLZ-00-12**	**10.0**	**16.1**	**14.4** [h]	**0.8**	**tr** [i]	**1.1**	**57.5**	**99.9**	**360**	**2.0**	**42.4**	0.33	**4.7**	**cc,bsp,pc,eq**
B2	**sph. clast** [j]	**LLZ-00-13**	**14.9**	**19.5**	**12.5**	**1.0**	**tr**	**1.0**	**51.1**	**100.0**	**416**	**100**	**48.9**	0.47	**6.4**	**sp,mfx,eq**
B3	**tuff**	**RC-KM-11**	**15.9**	**13.8**	**16.8**	**1.3**	**0.2**	**0.4**	**51.6**	**100.0**	**465**	**0.2**	**48.4**	0.52	**4.3**	**cc,pc,psp,ozs,eq**
Granite xenoliths in upper caldera-facies Hells Mesa Tuff and dome-derived tuff breccias: (granite xenoliths are not comagmatic with Hells Mesa Tuff)																
E4	san. granite	LLZ-00-8	20.9	46.6	15.8	1.1	tr	0.2	15.3	99.9	373	100	84.5	0.33	8.4	cat,mfx,mcg,grx,hg
E5	san. granite	LLZ-00-9A	20.4	50.8	20.6	2.9	0.3	0.5	4.5	100.0	378	100	95.5	0.29	12.1	hg,pmp,pks
T3	mic. granite	TS-4A	33.3	39.9 [k]	24.9	0.3	0.3 [l]	1.5	0.0	99.9	342	100	100	0.52	12.9	ag,per-om
Xenolith-poor zone of lower caldera-facies Hells Mesa Tuff (Thx):																
E6	tuff	RC-KM-19	11.8	14.7	10.5	2.2	tr	1.6	59.1	99.9	323	3.1	40.8	0.47	2.8	cc,eu,pc,eq
T4	tuff	TS-6	10.6	8.7	10.9	1.4	tr	0.8	67.6	100.0	364	1.6	32.4	0.54	2.2	cc,pc,eu,eq
B4	**tuff**	**LLZ-00-14**	**11.2**	**13.6**	**13.8**	**1.4**	**tr**	**0.7**	**59.3**	**100.0**	**423**	**0.9**	**40.7**	0.41	**4.1**	**cc,eu,pc,eq**

Notes: a) Magnetite includes some hematite; **b)** Sample E1 is slightly metasomatized; **c)** Sample E1 point counted 3 times to evaluate counting error; **d)** plagioclase slightly replaced by calcite; **e)** clast is 100% lithic; **f)** tr. is trace, < 0.1 %; **g)** Sample T2 is a lag-breccia clast of densely welded lower Hells Mesa Tuff containing 3.4 % andesite lithics; **h)** In K-metasomatized rocks plagioclase laths are replaced by adularia and clays, clays wash out of thin section so *euhedral holes* are counted as "plagioclase"; i) rhombic sphene is replaced by leucoxene and clays in metasomatized rocks; **j)** *sph. clast* is spherulitc (comagmatic) lithic fragment; k) microcline and orthoclase in this sample; l) monazite in this sample.

Textures: cc= cryptocrystalline groundmass, **mcg**= microcrystalline granular groundmass, **mcg-fb**= microcrystalline flow bands, **sp**= spherulitic groundmass, **psp**= patchy spherulites, **bsp**= broken spherulites, **pc**= pyroclastic (abundant broken crystal fragments), **eu**= eutaxitic, **mfx**= microfaulted crystals, **cat**= cataclastic (shattered crystals, slight rotations), **grx**= microgranulated crystals (counted as groundmass), **pks**= poikolitic sanidine with plagioclase inclusions, **hg**= hypidiomorphic granular, **ag**= allotriomorphic granular, **per-om**= perthitic orthoclase/microcline, **pmp**= partially melted plagioclase (cryptocrystalline pockets with birefringent reaction fronts), **ozs**= oscillatory zoned sanidine, **eq**= embayed quartz.

Table 2. Whole rock geochemical data for caldera-facies Hells Mesa Tuff and a comagmatic lava dome.

Oxides are in weight percent; elements in parts per million, ppm. LOI is loss on ignition (volatile content, wt. %). ND is not detected. nSiO_2 is *SiO2* normalized to 100% and volatile free.
Sample prefix indicates locality (Fig. 1): B is Bursum mine and E is Esperanza mine. Sample locations are shown on Figures 2-4. SeeTable 1 for rock type. K-metasomatized rocks shown in bold.

Sample	Field No	SiO_2	nSiO_2	TiO_2	Al_2O_3	Fe_2O_3	MnO	MgO	CaO	Na_2O	K_2O	P_2O_5	LOI	Total
Comagmatic lava dome (Tre) and dome-derived tuff breccias (Trt):(tuff breccias contain lava clasts)														
E1	LLZ-00-2	74.17	75.23	0.26	12.83	1.59	0.07	0.27	0.55	2.08	6.73 [a]	0.05	0.84	99.43
E2	LLZ-00-4	67.87 [b]	69.38	0.36	14.90	2.32	0.08	0.49	2.13 [b]	2.97	6.59	0.11	1.88	99.68
E3	LLZ-00-5	71.60	73.44	0.28	13.91	1.88	0.04	0.57	1.15	2.51	5.49	0.07	2.29	99.80
Granite xenolith in dome-derived tuff breccia: (granite xenolith is not comagmatic with Hells Mesa Tuff)														
E4	LLZ-00-8	75.04	75.63	0.20	12.79	1.31	0.03	0.26	0.68	2.98	5.87	0.05	0.50	99.72
Upper caldera-facies Hells Mesa Tuff (Thuf &Thu): (contains comagmatic-lithic lag-breccia clasts)														
B1	**LLZ-00-12**	**73.13 [c]**	**74.50**	**0.24**	**13.17**	**1.76**	**0.02**	**0.26**	**0.32**	**1.53**	**7.66**	**0.07**	**1.31**	**99.45**
B2	**LLZ-00-13**	**71.10**	**71.81**	**0.18**	**14.67**	**1.03**	**0.01**	**0.19**	**0.17**	**1.36**	**10.16**	**0.14**	**1.00**	**100.00**
B3	**RC-KM-11**	**72.57**	**74.01**	**0.24**	**13.44**	**1.80**	**0.02**	**0.38**	**0.25**	**1.02**	**8.27**	**0.07**	**1.63**	**99.69**
Xenolith-poor zone of lower caldera-facies Hells Mesa Tuff (Thx):														
B4	**LLZ-00-14**	**72.64**	**74.29**	**0.25**	**13.98**	**1.87**	**0.03**	**0.35**	**0.25**	**1.12**	**7.22**	**0.07**	**1.94**	**99.73**
E6	RC-KM-19	73.66	73.87	0.26	13.47	1.75	0.05	0.32	0.67	2.83	6.61	0.09	0.99	100.70

Sample	Field No	Cr	V	Ni	Cu	Zn	Ga	As	Rb	Sr	Y	Zr	Nb	Mo	Ba	Pb	Th	U
Comagmatic lava dome (Tre) and dome-derived tuff breccias (Trt):(tuff breccias contain lava clasts)																		
E1	LLZ-00-2	8	19	3	6	25	14	4	234	145	23	156	19	1	736	15	20	3
E2	LLZ-00-4	3	31	3	7	32	17	6	270	293	32	228	21	2	943	20	21	4
E3	LLZ-00-5	7	22	2	8	39	16	4	205	233	16	174	19	1	854	16	19	3
Granite xenolith in dome-derived tuff breccia: (granite xenolith is not comagmatic with Hells Mesa Tuff)																		
E4	LLZ-00-8	4	17	1	6	21	16	7	239	109	32	127	22	1	422	16	28	4
Upper caldera-facies Hells Mesa Tuff (Thuf &Thu): (contains comagmatic-lithic lag-breccia clasts)																		
B1	**LLZ-00-12**	**8**	**20**	**3**	**6**	**26**	**16**	**3**	**304**	**123**	**21**	**150**	**21**	**1**	**4009**	**20**	**25**	**2**
B2	**LLZ-00-13**	**3**	**9**	**1**	**9**	**21**	**17**	**3**	**427**	**63**	**22**	**118**	**24**	**1**	**418**	**17**	**39**	**2**
B3	**RC-KM-11**	**12**	**22**	**6**	**6**	**36**	**16**	**ND**	**345**	**100**	**16**	**156**	**22**	**ND**	**2461**	**16**	**24**	**4**
Xenolith-poor zone of lower caldera-facies Hells Mesa Tuff (Thx):																		
B4	**LLZ-00-14**	**9**	**19**	**4**	**7**	**81**	**19**	**12**	**334**	**88**	**18**	**161**	**25**	**1**	**686**	**19**	**28**	**5**
E6	RC-KM-19	4	16	5	7	31	16	11	321	145	19	152	20	ND	503	16	26	8

Notes: a) E1 is slightly metasomatized; b) E2 contains ~2% calcite, which slightly depresses SiO2 and exaggerates CaO relative to "true" values; c) SiO2 is not significantly affected by K-metasomatism (Dunbar, et al., 1994).
Data from NMT/NMBG XRF Lab, Chris McKee analyst.
Analytical methods as follows. Wavelength dispersive XRF spectrometry was used for major and trace element analyses. Major elements were analyzed with fused glass disks. Fused disks were prepared following the basic methods described by Norris and Hutton (1969). Approximately 1 g of sample was fused with 6 g of Sigma 12:22 flux, 50 mg of LiNO3, and 50 mg LiBr. Trace elements were determined on whole rock pressed powder pellets following Norrish and Chappell (1977). Seven grams of powdered sample were mixed with 7 drops of a 1% polyvinyl alcohol solution and pressed at ten tons with a boric acid backing.
The XRF lab at NMT/NMBG was partly funded by NSF grant EAR93-16467.

Table 3. Modal mineralogy (volume %) and maximum crystal size (mm) from a measured section of the Hells Mesa Tuff outflow sheet near Magdalena (Brown, 1972). Maximum crystal sizes measured by R. Chamberlin from archived thin sections provided by C.E. Chapin.

Sample	Fieldno	Q	A	P	MB	G	X	QF	XLMAX	STPOS
M18	M24-37	14.4	22.5	7.3	1.9	53.9	46.1	0.48	3.6	610
M17	M24-36	13.6	21.2	10.0	1.8	53.4	46.6	0.44	4.2	593
M16	M24-34	15.6	22.9	11.1	1.3	49.1	50.9	0.46	3.8	533
M15	M24-33	15.0	24.2	9.1	1.6	50.1	49.9	0.45	3.4	491
M14	M24-31	8.9	24.5	12.8	2.8	51.0	49.0	0.24	3.8	440
M13	M24-30	6.1	28.2	10.7	4.8	50.2	49.8	0.16	3.3	400
M12	M24-29	9.8	23.4	7.8	2.3	56.7	43.3	0.31		356
M11	M24-28	7.8	24.8	12.5	3.6	51.3	48.7	0.21	4.2	328
M10	M24-27	3.8	27.1	11.9	5.1	52.1	47.9	0.10	4.3	281
M9	M24-26	5.6	27.2	17.6	5.3	44.3	55.7	0.13	5.3	250
M8	M24-25	10.9	27.4	15.9	4.9	40.9	59.1	0.25		210
M7	M24-24	7.3	29.2	13.7	5.1	44.7	55.3	0.17	3.3	156
M6	M24-23	6.1	28.4	10.4	4.7	50.4	49.6	0.16	4.1	116
M5	M24-22	4.8	26.8	13.0	4.4	51.0	49.0	0.12		73
M4	M24-21	3.8	23.6	13.9	5.8	52.9	47.1	0.10	2.9	38
M3	M24-20	0.6	20.4	10.0	5.7	63.3	36.7	0.02	3.5	30
M2	M24-19	0.4	15.0	19.5	5.4	59.7	40.3	0.01	3.5	22
M1	M24-18	0.9	14.1	10.2	3.2	71.6	28.4	0.04	3.5	10

Notes: Q= quartz, A= sanidine (alkali feldspar) P= plagioclase, MB= magnetite/hematite plus biotite, G= groundmass (melt), X= total crystals, QF= quartz/total feldspar. XLMAX= maximum size of phenocrysts in thin section (mm)
STPOS= stratigraphic position, which is height above base (in feet).
Thin sections for samples M5, M8 and M12 not available to measure maximum crystal size.

Table 4. Modal mineralogy (volume %) and maximum crystal size (mm) for the entire Hells Mesa eruptive sequence.
Data from Brown, 1972 and this report (Table 1).

Sample	Fieldno	Q	A	P	MB	G	X	QF	XLMAX	STPOS
Comagmatic lava dome (Tre) and derivative tuff breccias (Trt):										
E1	LLZ002	9.4	20.9	13	2	54.5	45.5	0.28	6.9	23
E2	LLZ004	10.1	28.5	17	2.9	41.3	58.7	0.22	8.2	23
E3	LLZ005	16.5	25.4	12.3	3.7	42	58	0.44	5.8	23
Upper caldera-facies Hells Mesa Tuff (Thu & Thuf):										
T1	TS-2	14.7	16.6	14.2	2.1	52.4	47.6	0.48	3.7	21
B1	LLZ0012	10	16.1	14.4	1.9	57.5	42.5	0.33	4.7	21
B2	LLZ0013	14.9	19.5	12.5	2	51.2	48.8	0.47	6.4	21
B3	RCKM11	15.9	13.8	16.8	1.7	51.6	48.4	0.52	4.3	21
Xenolith-poor zone of lower caldera-facies Hells Mesa Tuff (Thx):										
E6	RCKM19	11.8	14.7	10.5	3.8	59.1	40.9	0.47	2.8	18
T2	TS-2A, clast	20.8	17.2	17.6	3.1	41.3	58.7	0.6	4.5	18
T4	TS-6	10.6	8.7	10.9	2.2	67.6	32.4	0.54	2.2	18
B4	LLZ0014	11.2	13.6	13.8	2.1	59.4	40.6	0.41	4.1	18
Outflow-facies Hells Mesa Tuff near Magdalena										
M18	M24-37	14.4	22.5	7.3	1.9	53.9	46.1	0.48	3.6	18
M17	M24-36	13.6	21.2	10	1.8	53.4	46.6	0.44	4.2	17
M16	M24-34	15.6	22.9	11.1	1.3	49.1	50.9	0.46	3.8	16
M15	M24-33	15	24.2	9.1	1.6	50.1	49.9	0.45	3.4	15
M14	M24-31	8.9	24.5	12.8	2.8	51	49	0.24	3.8	14
M13	M24-30	6.1	28.2	10.7	4.8	50.2	49.8	0.16	3.3	13
M12	M24-29	9.8	23.4	7.8	2.3	56.7	43.3	0.31		12
M11	M24-28	7.8	24.8	12.5	3.6	51.3	48.7	0.21	4.2	11
M10	M24-27	3.8	27.1	11.9	5.1	52.1	47.9	0.1	4.3	10
M9	M24-26	5.6	27.2	17.6	5.3	44.3	55.7	0.13	5.3	9
M8	M24-25	10.9	27.4	15.9	4.9	40.9	59.1	0.25		8
M7	M24-24	7.3	29.2	13.7	5.1	44.7	55.3	0.17	3.3	7
M6	M24-23	6.1	28.4	10.4	4.7	50.4	49.6	0.16	4.1	6
M5	M24-22	4.8	26.8	13	4.4	51	49	0.12		5
M4	M24-21	3.8	23.6	13.9	5.8	52.9	47.1	0.1	2.9	4
M3	M24-20	0.6	20.4	10	5.7	63.3	36.7	0.02	3.5	3
M2	M24-19	0.4	15	19.5	5.4	59.7	40.3	0.01	3.5	2
M1	M24-18	0.9	14.1	10.2	3.2	71.6	28.4	0.04	3.5	1

Notes: See Table 3 for explanation of abbreviations and Table 1 for lithology of caldera-facies samples. STPOS is *relative* stratigraphic position; top of outflow sheet (M18) is stratigraphically correlative to top of lower caldera-facies Hell Mesa Tuff

Table 5. Whole-rock major element data available for the Hells Mesa magmatic suite, n = 51 (continued on next page).
Includes intensely altered rocks and suspect analyses.

Sample	Field No	Map Unit	SiO2	TiO2	Al2O3	Fe2O3	MnO	MgO	CaO	Na2O	K2O	P2O5	LOI	Total	Reference
Comagmatic Hells Mesa-age lava dome and dome-derived tuffs:															
1 (E1)	LLZ-00-2	Tre	74.17	0.26	12.83	1.59	0.065	0.27	0.55	2.08	6.73	0.05	0.84	99.43	1
2 (E2)	LLZ-00-4	Trt (clast)	67.87	0.36	14.90	2.32	0.077	0.49	2.13	2.97	6.59	0.11	1.88	99.68	1
3 (E3)	LLZ-00-5	Trt	71.60	0.28	13.91	1.88	0.035	0.57	1.15	2.51	5.49	0.07	2.29	99.80	1
Upper caldera-facies Hells Mesa Tuff (contains comagatic lag breccias):															
4 (B1)	LLZ-00-12	Thuf	73.13	0.24	13.17	1.76	0.020	0.26	0.32	1.53	7.66	0.07	1.31	99.45	1
5 (B2)	LLZ-00-13	Thuf (clast	71.10	0.18	14.67	1.03	0.013	0.19	0.17	1.36	10.16	0.14	1.00	100.00	1
6 (B3)	RC-KM-11	Thu	72.57	0.24	13.44	1.80	0.020	0.38	0.25	1.02	8.27	0.07	1.63	99.69	2
xenolith-poor zone of lower caldera-facies Hells Mesa Tuff															
7 (E6)	RC-KM-19	Thx	73.66	0.26	13.47	1.75	0.050	0.32	0.67	2.83	6.61	0.09	0.99	100.70	2
8 (B4)	LLZ-00-14	Thx	72.64	0.25	13.98	1.87	0.030	0.35	0.25	1.12	7.22	0.07	1.94	99.73	1
Caldera-facies Hells Mesa Tuff and clasts of Hells Mesa Tuff in younger formations:															
9	82-4-15-1	Thm	72.87	0.23	13.31	1.65	0.040	0.28	0.32	2.14	8.21	0.07	0.65	99.77	3
10	82-4-15-2	Thm	69.71	0.27	13.95	2.02	0.060	0.35	1.87	2.48	6.88	0.08	1.85	99.52	3
11	82-4-15-3	Thm	73.17	0.26	13.40	1.98	0.020	0.29	0.32	1.23	8.45	0.08	0.44	99.64	3
12	82-4-15-5	Thm	74.48	0.23	12.79	1.99	0.070	0.14	0.30	3.15	6.29	0.09	0.63	100.16	3
13	4-18-82-9	Thx?	69.30	0.29	14.79	2.14	0.070	0.56	0.40	1.67	8.07	0.09	1.12	98.50	3
14	4-18-82-10	Thx?	71.81	0.25	13.28	1.94	0.040	0.62	1.17	2.83	4.89	0.07	1.27	98.17	3
15	4-18-82-12	Thm	72.54	0.23	13.32	1.84	0.030	0.37	0.37	2.41	7.90	0.07	0.87	99.95	3
16	4-18-82-14	Thx?	69.96	0.27	14.18	1.98	0.050	0.56	1.61	3.83	5.24	0.08	0.78	98.54	3
17	4-18-82-15	Thx?	71.93	0.23	13.53	1.66	0.090	0.37	0.72	2.63	6.60	0.06	0.58	98.40	3
18	4-18-82-17	Thx?	71.88	0.23	14.18	1.55	0.030	0.41	0.93	3.33	6.84	0.07	0.49	99.94	3
19	82-4-15-6	Thm/r	72.09	0.34	13.14	2.75	0.007	0.34	0.51	3.35	6.09	0.12	0.63	99.37	3
20	4-18-82-1	Thm/r	74.96	0.18	12.74	1.40	0.007	0.30	0.38	2.60	6.47	0.05	0.27	99.36	3
21	4-18-82-2	Thm/r	72.05	0.32	14.10	1.53	0.001	0.31	0.67	2.84	7.33	0.12	0.38	99.65	3
22	4-18-82-3	Thm/r	71.79	0.37	13.78	2.89	0.006	0.43	0.54	3.38	5.81	0.15	0.44	99.59	3
23	4-18-82-4	Thm/r	72.10	0.29	13.53	2.13	0.004	0.33	0.42	3.48	5.61	0.10	0.73	98.72	3
24	4-18-82-5	Thm/r	73.88	0.33	13.28	2.41	0.002	0.23	0.38	2.18	5.81	0.12	1.02	99.64	3
25	4-18-82-6	Thm/r	72.33	0.34	13.23	2.80	0.001	0.27	0.47	3.20	6.18	0.13	0.69	99.64	3
26	4-18-82-8	Thm/r	71.96	0.30	13.61	2.33	0.001	0.24	0.43	2.98	5.30	0.10	0.84	98.09	3
27	4-18-82-11	Thm/r	70.83	0.31	13.81	2.42	0.005	0.33	0.50	3.16	5.84	0.10	0.75	98.06	3
28	4-18-82-16	Thm/r	72.65	0.33	13.76	2.33	0.005	0.20	0.53	3.85	6.00	0.12	0.53	100.31	3
29	KM-54	Tzt clast	72.79	0.27	13.26	2.22	0.080	0.37	0.79	1.42	7.83	0.05	0.15	99.23	4
30	KM-58	Tzt clast	72.80	0.30	14.47	2.18	0.020	0.64	0.36	0.99	8.39	0.05	0.18	100.38	4
31	KM-59	Tzt clast	74.96	0.24	14.03	1.77	0.020	0.41	0.28	1.26	7.27	0.04	0.18	100.46	4
32	KM-60	Thx?	72.36	0.26	13.53	1.98	0.090	0.48	1.79	1.67	7.18	0.05	0.33	99.72	4
33*	KM-61	Thx?	75.90	0.22	13.30	1.85	0.060	0.35	0.61	2.53	6.28	0.04	0.06	101.20	4
34	KM-96	Tzt clast	74.52	0.24	12.92	1.61	0.010	0.23	0.17	0.60	8.52	0.06	1.06	99.94	4
35	KM-102	Tzt clast	73.03	0.25	13.34	1.62	0.010	0.21	0.22	0.71	8.86	0.06	1.21	99.52	4
36	KM-112	Tpfm clast	73.38	0.26	13.25	1.99	0.050	0.33	0.27	1.12	7.60	0.07	1.73	100.05	4
37	KM-113	Tpfm clast	71.18	0.29	14.11	2.11	0.050	0.29	0.46	1.63	7.69	0.08	1.59	99.48	4
38	KM-114	Tpfm clast	71.81	0.28	13.77	2.01	0.040	0.28	0.43	1.16	8.79	0.08	1.78	100.43	4
39	KM-115	Tpfm clast	73.33	0.23	13.13	1.55	0.050	0.27	0.20	0.80	8.49	0.06	1.56	99.67	4
40	KM-116	Tpfm clast	73.51	0.24	13.07	1.85	0.050	0.25	0.44	2.00	6.79	0.07	1.36	99.63	4
41	KM-117	Tpf clast	71.65	0.41	13.41	2.81	0.040	0.45	0.86	2.29	6.23	0.13	1.47	99.75	4
42	KM-118	Tpf clast	73.95	0.22	12.91	1.65	0.070	0.44	0.69	2.85	5.82	0.07	0.87	99.54	4
43	KM-119	Tpf clast	74.11	0.22	13.00	1.65	0.040	0.30	0.50	2.18	6.37	0.06	1.43	99.86	4
44	KM-120	Tpf clast	73.47	0.25	13.78	1.77	0.040	0.23	0.90	3.14	5.70	0.07	0.84	100.19	4
45	KM-121	Tpf clast	74.37	0.21	12.87	1.59	0.030	0.30	0.64	2.66	5.62	0.06	1.23	99.58	4
46	KM-153	Thm	77.27	0.16	11.33	1.09	0.030	0.08	0.10	0.83	8.74	0.02	0.66	100.31	4
47	KM-155	Thm	78.47	0.15	11.88	1.13	0.010	0.34	0.04	0.11	5.83	0.03	2.45	100.44	4
48	KM-158	Thm	75.54	0.21	13.00	1.50	0.030	0.39	0.53	2.61	5.10	0.05	1.32	100.28	4
Hells Mesa Tuff (outflow facies)															
49	19-D	Th	69.84	0.37	15.12	2.26	0.040	0.72	1.84	3.90	4.47	0.11	0.92	99.59	4
50	LJ4	Th(lower)	69.34	0.22	14.75	2.39	0.033	0.65	1.63	3.85	4.40	0.09	2.09	99.44	4&5
51*	LJ17	Th(top)	77.60	0.12	10.53	0.98	0.540	0.23	0.69	2.18	5.14	0.02	1.61	99.64	5

NOTES: Oxides in weight percent. ND = not detected; na = not analysed. Distinctly anomalous values are highlighted.
Samples: K-metasomatized samples are shown in bold; hydrothermally altered and mineralized samples in italics, and supect analyses are marked with an asterisk (# 33 & 51).
Map units: see Fig. 5 for explanation of most map units. Additional units: Thm/r, r is for red zone of Eggleston et al.,1983; Th is outflow Hells MesaTuff ;
Tzt is medial tuff of Luis Lopez Fm.; Tpf is Popotosa Fm. fanglomerate facies: and Tpfm is metasomatized Popotosa fanglomerate facies.
References: 1 = this report (Table 2); 2 = Chamberlin et al., 2004; 3 = Eggleston et al. 1983; 4 = Ennis, 1996; 5 = Spradlin, 1976.
Highlighted sample numbers are excluded in calculation of mean SiO2 content of Hells Mesa rocks and construction of SiO2 histogram.

Table 6. Whole-rock trace element data available for the Hells Mesa magmatic suite (n = 51).
Includes intensely altered rocks and suspect analyses.

Sample	Field No	Map Unit	Cr	V	Ni	Cu	Zn	Ga	As	Rb	Sr	Y	Zr	Nb	Mo	Ba	Pb	Th	U	Reference
Comagmatic Hells Mesa-age lava dome and dome-derived tuffs:																				
1 (E1)	LLZ-00-2	Tre	8	19	3	6	25	14	4	234	145	23	156	19	1	736	15	20	3	1
2 (E2)	LLZ-00-4	Trt (clast)	3	31	3	7	32	17	6	270	293	32	228	21	2	943	20	21	4	1
3 (E3)	LLZ-00-5	Trt	7	22	2	8	39	16	4	205	233	16	174	19	1	854	16	19	3	1
Upper caldera-facies Hells Mesa Tuff (contains comagatic lag breccias):																				
4 (B1)	LLZ-00-12	Thuf	8	20	3	6	26	16	3	304	123	21	150	21	1	4009	20	25	2	1
5 (B2)	LLZ-00-13	Thuf (clast)	3	9	1	9	21	17	3	427	63	22	118	24	1	418	17	39	2	1
6 (B3)	RC-KM-11	Thu	12	22	6	6	36	16	ND	345	100	16	156	22	ND	2461	16	24	4	2
xenolith-poor zone of lower caldera-facies Hells Mesa Tuff																				
7 (E6)	RC-KM-19	Thx	4	16	5	7	31	16	11	321	145	19	152	20	ND	503	16	26	8	2
8 (B4)	LLZ-00-14	Thx	9	19	4	7	81	19	12	334	88	18	161	25	1	686	19	28	5	1
Caldera-facies Hells Mesa Tuff and clasts of Hells Mesa Tuff in younger formations:																				
9	82-4-15-1	Thm	na	na	na	11	37	na	na	424	89	24	145	27	na	219	18	38	6	3
10	82-4-15-2	Thm	na	na	na	5	43	na	na	429	247	31	225	30	na	339	12	34	5	3
11	82-4-15-3	Thm	na	na	na	12	30	na	na	383	88	23	155	23	na	159	27	29	4	3
12	82-4-15-5	Thm	na	na	na	37	85	na	na	308	216	26	137	22	na	150	40	30	3	3
13	4-18-82-9	Thx?	na	na	na	9	36	na	na	416	133	26	174	25	na	349	20	30	3	3
14	4-18-82-10	Thx?	na	na	na	4	20	na	na	223	170	21	133	23	na	190	12	30	5	3
15	4-18-82-12	Thm	na	na	na	3	13	na	na	372	122	19	146	24	na	249	9	26	3	3
16	4-18-82-14	Thx?	na	na	na	9	31	na	na	227	276	25	128	24	na	309	17	26	6	3
17	4-18-82-15	Thx?	na	na	na	4	24	na	na	338	153	21	170	27	na	209	18	35	6	3
18	4-18-82-17	Thx?	na	na	na	10	20	na	na	304	191	24	144	25	na	259	12	29	5	3
19	82-4-15-6	Thm/r	na	na	na	8	113	na	na	317	214	23	143	23	na	155	26	29	3	3
20	4-18-82-1	Thm/r	na	na	na	18	93	na	na	335	177	17	112	26	na	409	25	33	4	3
21	4-18-82-2	Thm/r	na	na	na	12	10	na	na	292	260	22	136	23	na	185	23	28	4	3
22	4-18-82-3	Thm/r	na	na	na	10	173	na	na	298	224	22	145	22	na	185	30	27	4	3
23	4-18-82-4	Thm/r	na	na	na	22	125	na	na	366	217	22	142	24	na	184	31	31	3	3
24	4-18-82-5	Thm/r	na	na	na	9	143	na	na	301	137	24	140	22	na	140	30	30	5	3
25	4-18-82-6	Thm/r	na	na	na	14	75	na	na	323	217	24	144	23	na	160	49	29	4	3
26	4-18-82-8	Thm/r	na	na	na	7	50	na	na	255	142	23	148	24	na	140	16	33	6	3
27	4-18-82-11	Thm/r	na	na	na	9	78	na	na	272	168	23	145	24	na	170	16	32	6	3
28	4-18-82-16	Thm/r	na	na	na	na	na	na	na	304	330	18	129	17	na	na	na	28	4	3
29	KM-54	Tzt clast	562	na	na	na	33	na	9	424	120	60	444	23	na	794	26	19	4	4
30	KM-58	Tzt clast	268	na	na	na	74	na	16	310	16	61	152	28	na	998	34	27	5	4
31	KM-59	Tzt clast	510	na	na	na	52	na	13	341	77	20	157	31	na	600	19	30	10	4
32	KM-60	Thx?	461	na	na	na	30	na	6	335	92	21	138	26	na	511	17	26	9	4
33*	KM-61	Thx?	641	na	na	na	45	na	10	305	117	17	134	29	na	502	29	29	9	4
34	KM-96	Tzt clast	26	na	3	11	52	15	11	311	88	22	134	23	2	858	182	25	8	4
35	KM-102	Tzt clast	19	na	3	11	52	15	11	311	98	25	151	23	2	1187	327	22	5	4
36	KM-112	Tpfm clast	144	na	7	9	69	16	18	372	75	21	140	22	8	773	39	25	6	4
37	KM-113	Tpfm clast	165	na	6	9	56	16	8	328	144	28	175	22	9	1622	28	22	5	4
38	KM-114	Tpfm clast	134	na	3	6	59	16	8	375	111	26	158	22	7	1586	29	20	4	4
39	KM-115	Tpfm clast	137	na	5	10	44	16	10	419	74	28	136	25	7	1911	36	30	7	4
40	KM-116	Tpfm clast	151	na	5	3	39	16	5	340	110	22	135	23	9	636	16	27	6	4
41	KM-117	Tpf clast	171	na	8	11	45	17	8	353	214	27	159	19	8	1742	33	21	6	4
42	KM-118	Tpf clast	182	na	5	3	32	15	12	291	151	18	127	24	11	1044	58	29	5	4
43	KM-119	Tpf clast	190	na	10	5	35	16	11	330	147	22	129	23	10	2073	24	28	5	4
44	KM-120	Tpf clast	148	na	6	6	28	16	8	261	230	21	155	24	9	2274	29	26	5	4
45	KM-121	Tpf clast	177	na	3	8	31	16	6	297	171	20	126	24	11	1362	25	29	6	4
46	KM-153	Thm	227	26	6	7	18	14	9	306	27	64	155	28	11	275	17	22	6	4
47	KM-155	Thm	144	24	5	10	34	17	5	277	40	18	108	22	8	598	278	29	8	4
48	KM-158	Thm	129	na	6	3	24	15	3	251	118	19	119	24	7	473	19	30	5	4
Hells Mesa Tuff (outflow facies)																				
49	19-D	Th	na	na	na	na	na	na	na	144	384	27	219	26	na	1028	na	18	3	4
50	LJ4	Th(lower)	na	na	na	na	na	na	na	169	249	34	219	na	na	1063	na	17	4	4&5
51*	LJ17	Th(top)	na	na	na	na	na	na	na	na	na	na	na	na	na	na	na	na	na	5

NOTES: Elements in parts per million, ppm. ND = not detected; na = not analysed. Distinctly anomalous values are highlighted.
Samples: K-metasomatized samples are shown in bold; hydrothermally altered and mineralized samples in italics, and supect analyses are marked with an asterisk (# 33 & 51) .
Map units: see Fig. 5 for explanation of most map units. Additional units: Thm/r, r is for red zone of Eggleston et al.,1983; Th is outflow Hells MesaTuff ;
Tzt is medial tuff of Luis Lopez Fm.; Tpf is Popotosa Fm. fanglomerate facies: and Tpfm is metasomatized Popotosa fanglomerate facies.
References: 1 = this report (Table 2); 2 = Chamberlin et al., 2004; 3 = Eggleston et al. 1983; 4 = Ennis, 1996; 5 = Spradlin, 1976.
Highlighted sample numbers are excluded in calculation of mean SiO_2 content of Hells Mesa rocks and construction of SiO_2 histogram.

Table 7. Normalized whole-rock geochemical data for unaltered or slightly altered samples of Hells Mesa Tuff and a comagmatic lava dome (n = 11).
All data normalized to 100% and volatile free. Includes calculated mean values and standard deviations.

Sample	Field No	Map Unit	SiO2	TiO2	Al2O3	Fe2O3	MnO	MgO	CaO	Na2O	K2O	P2O5	LOI	Total	Reference
Comagmatic Hells Mesa-age lava dome and dome-derived tuffs															
1 (E1)	LLZ-00-2	Tre	75.23	0.26	13.01	1.61	0.07	0.27	0.56	2.11	6.83	0.05	0.00	100.00	1
2 (E2)	LLZ-00-4	Trt (clast)	69.38	0.37	15.23	2.37	0.08	0.50	2.18	3.04	6.74	0.11	0.00	100.00	1
3 (E3)	LLZ-00-5	Trt	73.44	0.29	14.27	1.93	0.04	0.58	1.18	2.57	5.63	0.07	0.00	100.00	1
Lower caldera-facies Hells Mesa Tuff (xenolith bearing)															
7 (E6)	RC-KM-19	Thx	73.66	0.26	13.51	1.76	0.05	0.32	0.67	2.84	6.63	0.09	0.00	100.00	2
10	82-4-15-2	Thm	71.38	0.28	14.28	2.07	0.06	0.36	1.91	2.54	7.04	0.08	0.00	100.00	3
14	4-18-82-10	Thx?	74.11	0.26	13.70	2.00	0.04	0.64	1.21	2.92	5.05	0.07	0.00	100.00	3
16	4-18-82-14	Thx?	71.56	0.28	14.50	2.03	0.05	0.57	1.65	3.92	5.36	0.08	0.00	100.00	3
17	4-18-82-15	Thx?	73.52	0.24	13.83	1.70	0.09	0.38	0.74	2.69	6.75	0.06	0.00	100.00	3
18	4-18-82-17	Thx?	72.27	0.23	14.26	1.56	0.03	0.41	0.94	3.35	6.88	0.07	0.00	100.00	3
Hells Mesa Tuff (outflow facies)															
49	19-D	Th	70.80	0.37	15.32	2.29	0.04	0.73	1.86	3.95	4.53	0.11	0.00	100.00	4
50	LJ4	Th(lower)	71.23	0.23	15.15	2.45	0.03	0.67	1.67	3.95	4.52	0.09	0.00	99.99	4&5
		MEAN:	72.4	0.28	14.28	1.98	0.05	0.49	1.24	3.08	6.00	0.08			
		STD. DEV.	± 1.74	± 0.05	± 0.74	± 0.30	± 0.02	± 0.15	± 0.51	± 0.63	± 0.99	± 0.02			

Sample	Field No	Map Unit	Cr	V	Ni	Cu	Zn	Ga	As	Rb	Sr	Y	Zr	Nb	Mo	Ba	Pb	Th	U
Comagmatic Hells Mesa-age lava dome and dome-derived tuffs																			
1 (E1)	LLZ-00-2	Tre	8	19	3	6	25	14	4	234	145	23	156	19	1	736	15	20	3
2 (E2)	LLZ-00-4	Trt (clast)	3	31	3	7	32	17	6	270	293	32	228	21	2	943	20	21	4
3 (E3)	LLZ-00-5	Trt	7	22	2	8	39	16	4	205	233	16	174	19	1	854	16	19	3
Lower caldera-facies Hells Mesa Tuff (xenolith bearing)																			
7 (E6)	RC-KM-19	Thx	4	16	5	7	31	16	11	321	145	19	152	20	ND	503	16	26	8
10	82-4-15-2	Thm	na	na	na	5	43	na	na	429	247	31	225	30	na	339	12	34	5
14	4-18-82-10	Thx?	na	na	na	4	20	na	na	223	170	21	133	23	na	190	12	30	5
16	4-18-82-14	Thx?	na	na	na	9	31	na	na	227	276	25	128	24	na	309	17	26	6
17	4-18-82-15	Thx?	na	na	na	4	24	na	na	338	153	21	170	27	na	209	18	35	6
18	4-18-82-17	Thx?	na	na	na	10	20	na	na	304	191	24	144	25	na	259	12	29	5
Hells Mesa Tuff (outflow facies)																			
49	19-D	Th	na	na	na	na	na	na	na	144	384	27	219	26	na	1028	na	18	3
50	LJ4	Th(lower)	na	na	na	na	na	na	na	169	249	34	219	na	na	1063	na	17	4
		MEAN:	5.5	22	3.3	6.7	29.4	15.8	4.7	260	226	25	177	23.4	1.3	585	15.3	25	4.4
		STD. DEV.	± 2.4	± 6	± 1.3	± 2.1	± 8.0	± 1.3	± 1.1	± 83	± 75	± 6	± 39	± 3.7	± 0.6	± 346	± 2.9	± 6.4	± 1.2

Notes: Oxides in weight percent. Elements in parts per million, ppm. ND= not detected; na= not analysed. Distinctly anomalous values (highlighted) are not included in calculated means. Sample numbers as in Table 5.
Map units: Tre= Hell Mesa-age lava dome, Trt= dome-derived tuffs, Thx = xenolith-poor, lower caldera-facies Hells Mesa Tuff; Thm = lower xenolith-rich mesobreccia; Th = outflow Hells Mesa.
References: 1 = this report; 2 = Chamberlin et al., 2004; 3 = Eggleston et al. 1983; 4 = Ennis, 1996; 5 = Spradlin, 1976.

Table 8. Whole-rock geochemical data for post-Hells-Mesa rhyolite units (30.0-28.7 Ma) erupted from vent areas within and adjacent to the eastern Socorro caldera.

Sample	Field No	Map Unit	SiO2	TiO2	Al2O3	Fe2O3	MnO	MgO	CaO	Na2O	K2O	P2O5	LOI	Total	Reference
R1	LLZ-43	Tj	69.51	0.54	15.22	2.29	0.08	0.24	0.57	4.65	6.44	0.09	0.51	100.13	2
R2	LLZ-99-11	Tj	68.90	0.51	15.13	2.24	0.08	0.23	0.60	4.70	6.19	0.09	0.61	99.28	1
R3	LLZ-99-4	Tzu	74.45	0.23	12.89	1.32	0.03	0.20	0.75	3.37	5.58	0.08	0.85	99.75	2
R4	LLZ-99-5F	Tzu	74.02	0.22	13.46	1.27	0.04	0.17	0.62	3.16	6.38	0.08	0.79	100.22	2
R5	SOC-99-1	Tzu	77.27	0.19	11.40	1.03	0.01	0.10	0.25	2.05	6.85	0.04	1.01	100.20	2
R6	LLZ-44	Tzt	70.77	0.23	11.12	1.52	0.02	0.81	2.68	0.85	3.44	0.06	8.90	100.41	2
R7	**LLZ-12**	**Tzt**	**73.29**	**0.23**	**12.62**	**1.26**	**0.04**	**0.34**	**0.58**	**0.17**	**9.60**	**0.07**	**2.15**	**100.35**	2

Sample	Field No	Map Unit	Cr	V	Ni	Cu	Zn	Ga	As	Rb	Sr	Y	Zr	Nb	Mo	Ba	Pb	Th	U
R1	LLZ-43	Tj	5	13	5	4	54	21	6	142	16	50	735	20	1	133	13	14	4
R2	LLZ-99-11	Tj	ND	19	4	5	74	21	3	144	30	50	722	26	3	181	19	19	4
R3	LLZ-99-4	Tzu	8	15	4	8	29	17	4	183	220	13	148	16	ND	830	19	24	6
R4	LLZ-99-5F	Tzu	7	17	4	9	26	17	4	213	202	13	147	17	ND	889	32	26	8
R5	SOC-99-1	Tzu	7	11	4	4	13	15	4	204	138	12	145	15	ND	712	22	21	4
R6	LLZ-44	Tzt	11	16	7	10	25	14	5	210	1734	11	106	9	ND	192	14	23	5
R7	**LLZ-12**	**Tzt**	**18**	**15**	**10**	**8**	131	**14**	**6**	**342**	**41**	**20**	**121**	**17**	ND	**617**	**10**	**22**	**6**

Notes: Oxides in weight percent. Elements in parts per million, ppm. ND is not detected; na is not analysed. Distinctly anomalous values are highlighted.
K-metasomatized samples shown in bold.

Map units: Tj = La Jencia Tuff; Tzu = upper rhyolite member of Luis Lopez Fm.; Tzt = medial pumiceous tuff member of Luis Lopez Fm. **References:** 1 = this report (Table 2); 2 = Chamberlin et al.,2004

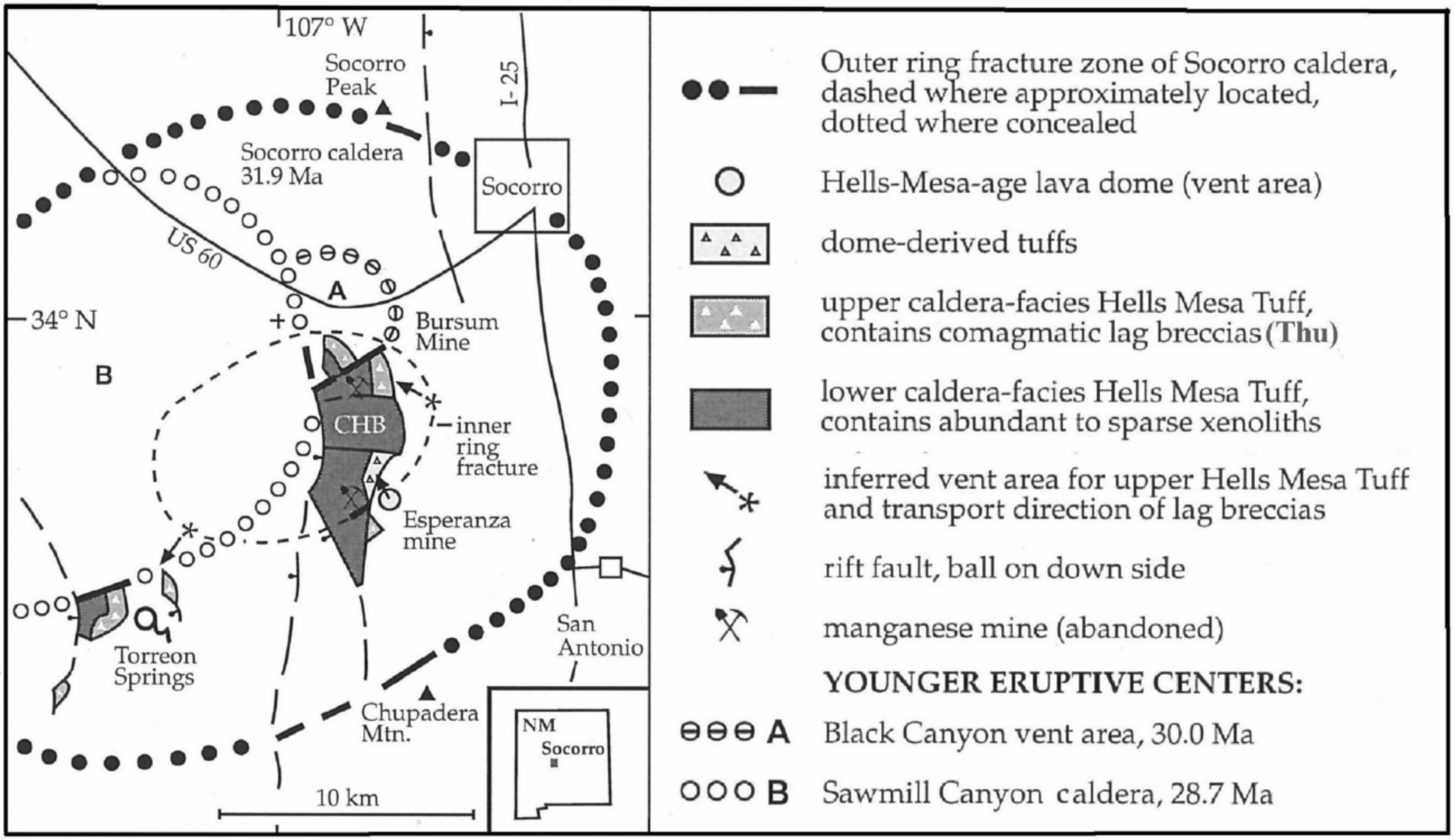

Figure 1. Structural index map of the eastern Socorro caldera. Generalized from Chamberlin et al., 2004; Osburn et al., 1986, and this report (Figs. 2–4). CHB is a magmatically uplifted central horst block.

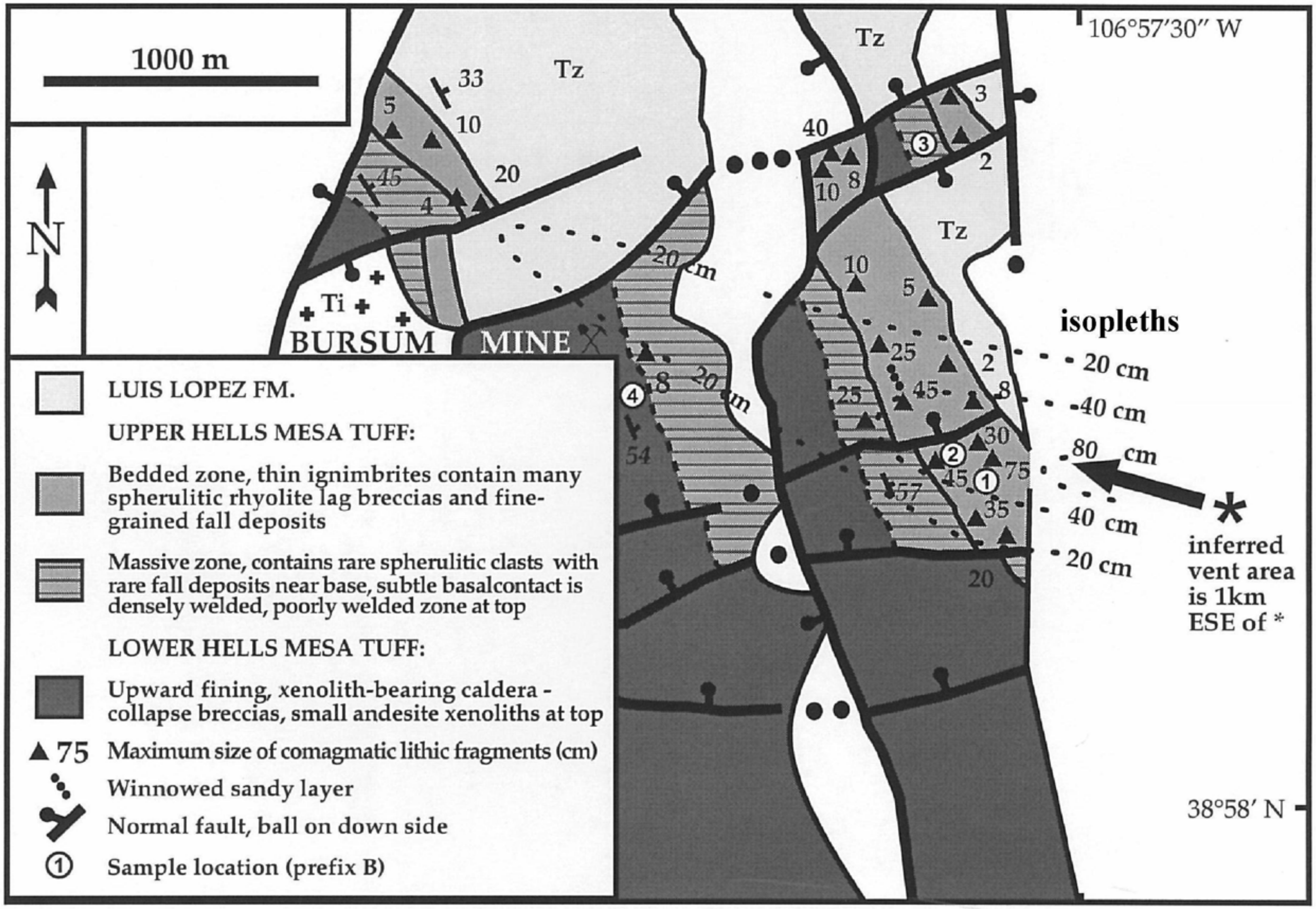

Figure 2. Geologic map of the Bursum mine area. Modified after Chamberlin et al., 2002. White areas are post-Luis Lopez age strata, mostly Santa Fe Group basin-fill deposits.

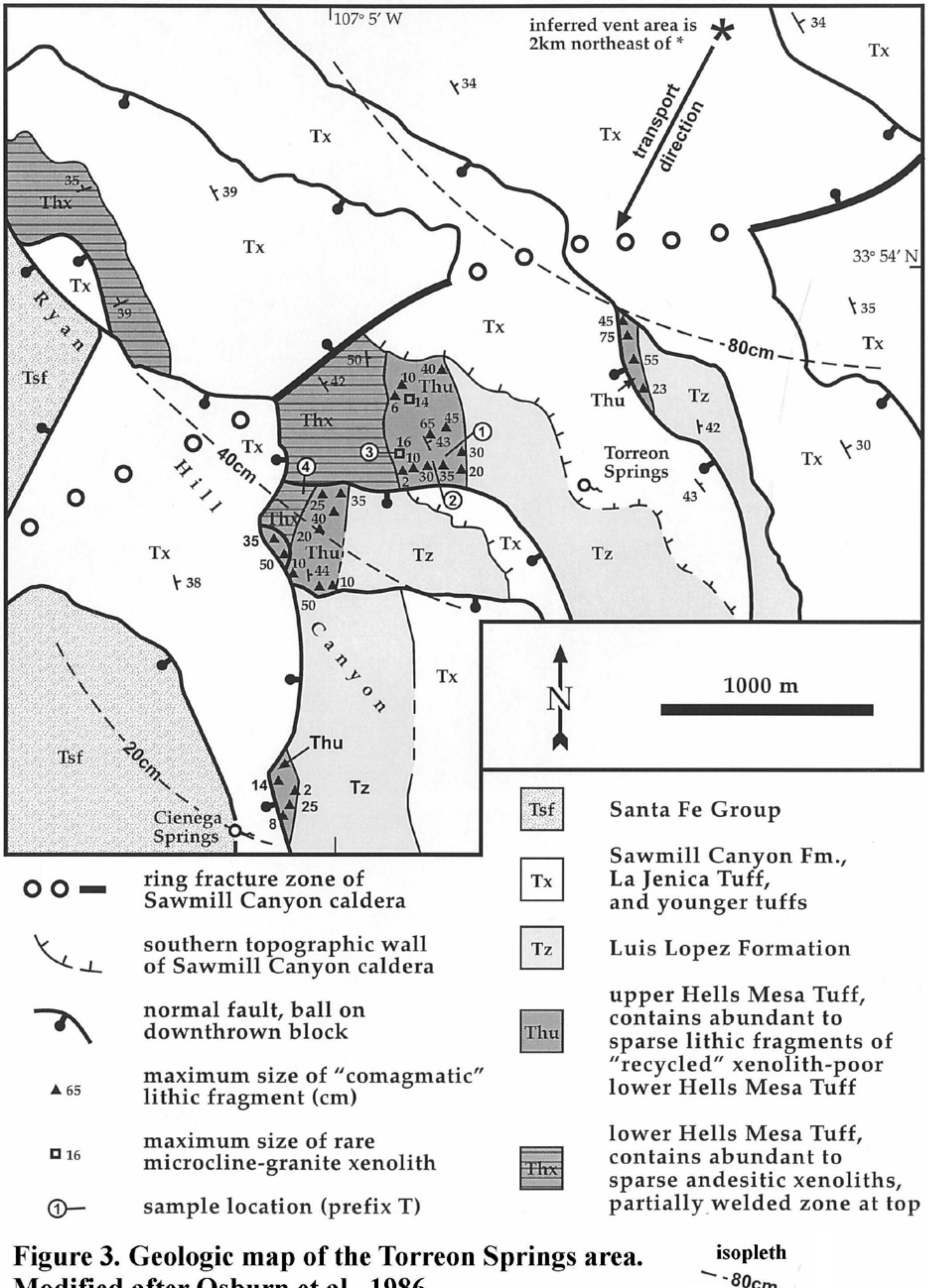

Figure 3. Geologic map of the Torreon Springs area. Modified after Osburn et al., 1986.

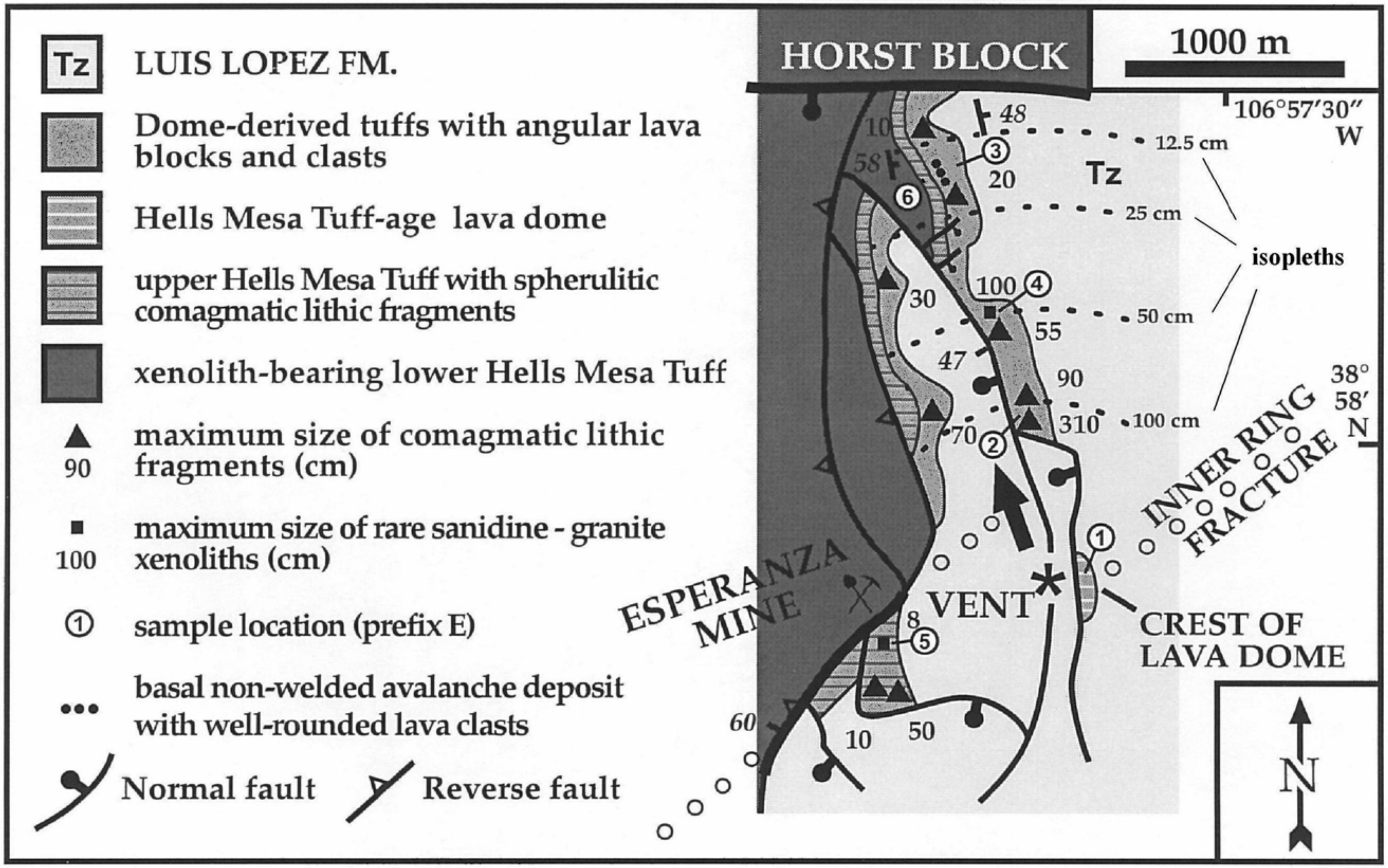

Figure 4. Geologic map of the Esperanza Mine area. Modified after Chamberlin et al., 2002.

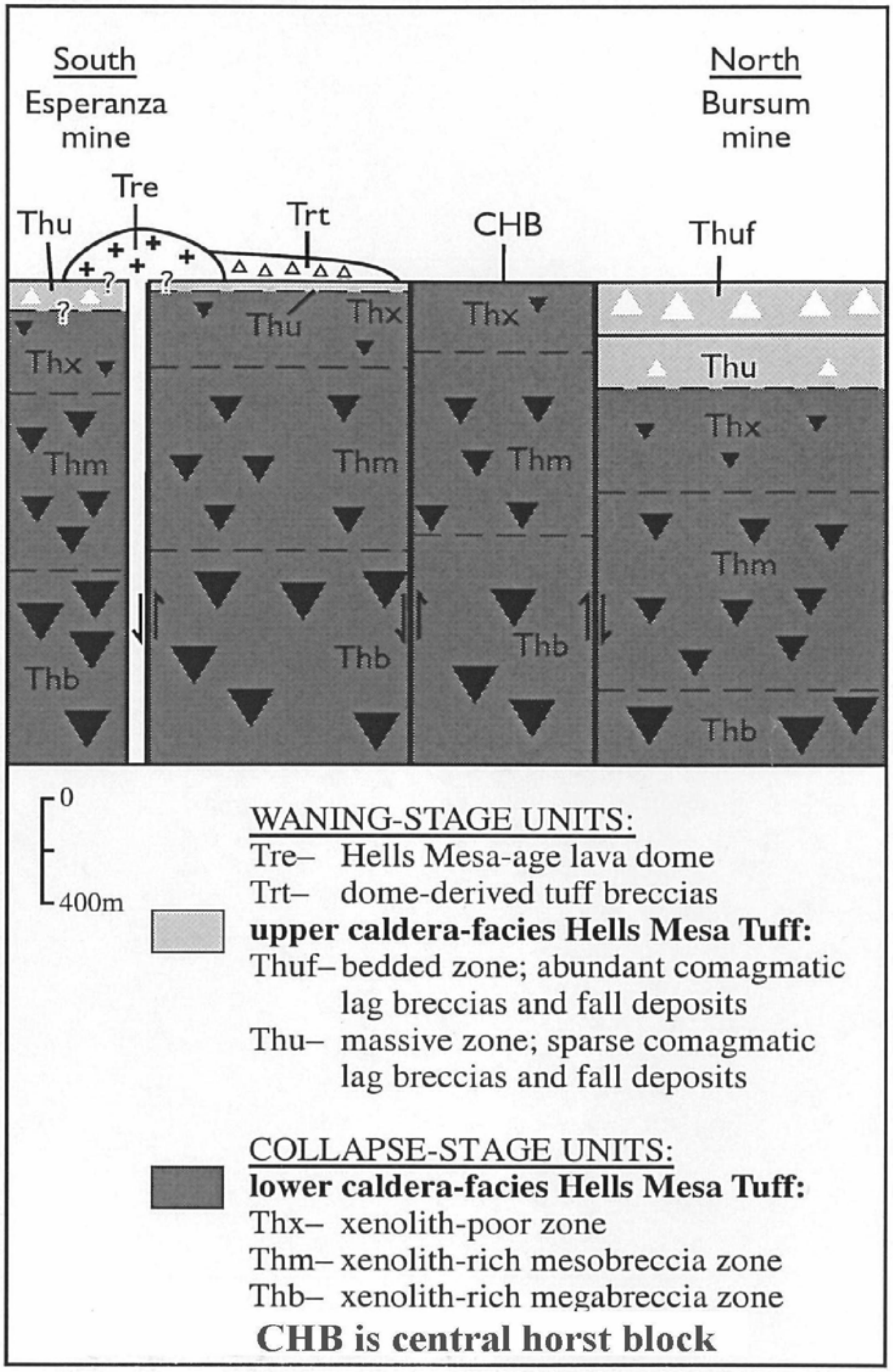

Figure 5. Schematic stratigraphic section of the Hells Mesa facies in the eastern Socorro caldera. Modified after Chamberlin et al.,2002. Contacts are dashed where gradational, solid at cooling breaks, and queried where not exposed. The Torreon Springs facies of the upper Hells Mesa Tuff occupies the same stratigraphic position as the upper bedded zone east of the Bursum mine (Thuf). This figure supersedes a similar figure shown as fig. 2 in Chamberlin, 2001b.

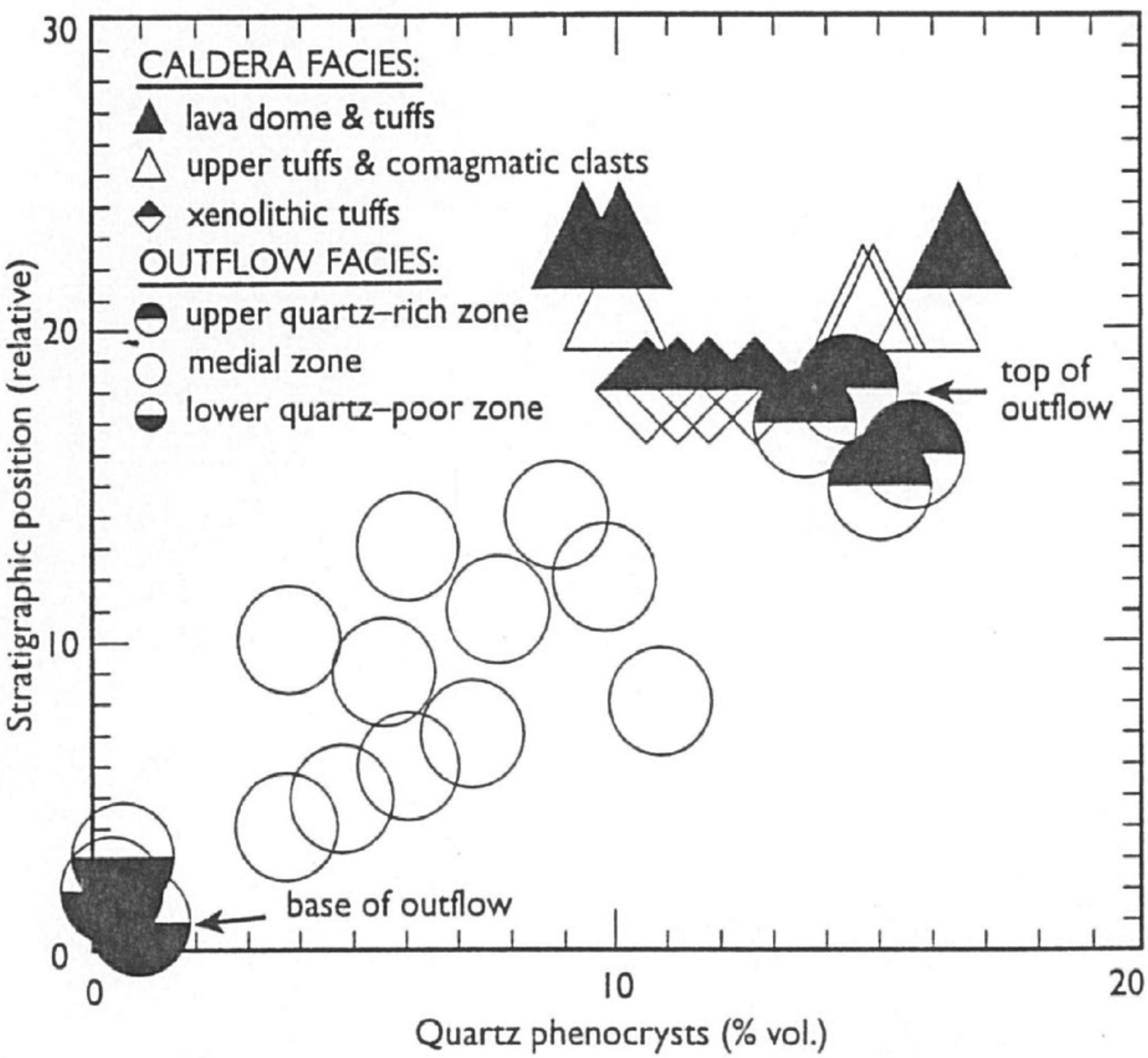

Figure 6. Quartz content vs. relative stratigraphic position or the Hells Mesa eruptive sequence.
Data from Brown (1972) and Table 1.
Symbol size reflects a counting error of ±10%.

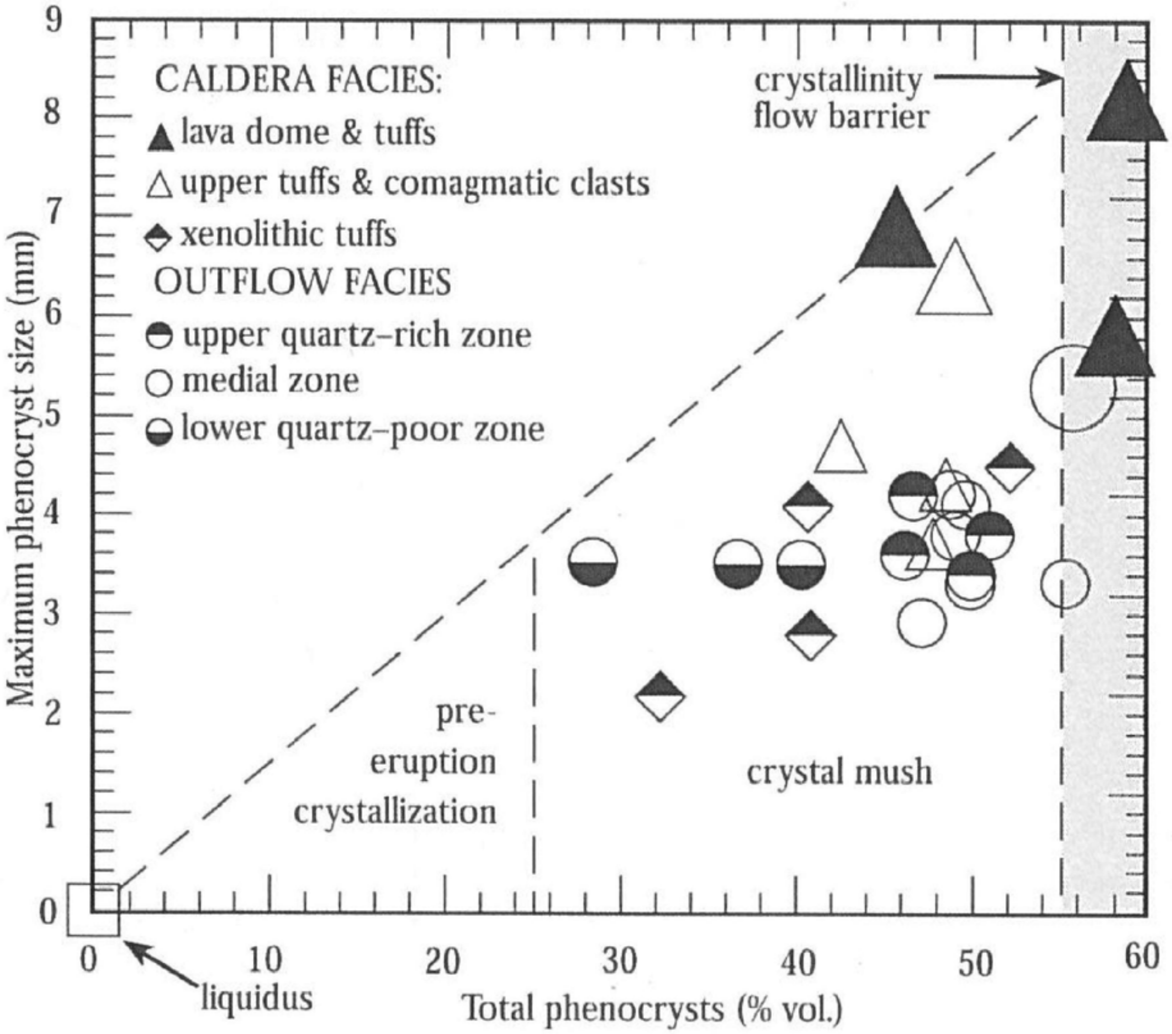

Figure 7. Maximum crystal size vs. crystallinity for the Hells Mesa eruptive sequence. Data from Tables 1 and 3. Crystallinity-flow barrier from Marsh (1981). Symbol size reflects ±2% counting error for medium-grained samples and ±5% counting error for coarse-grained samples.

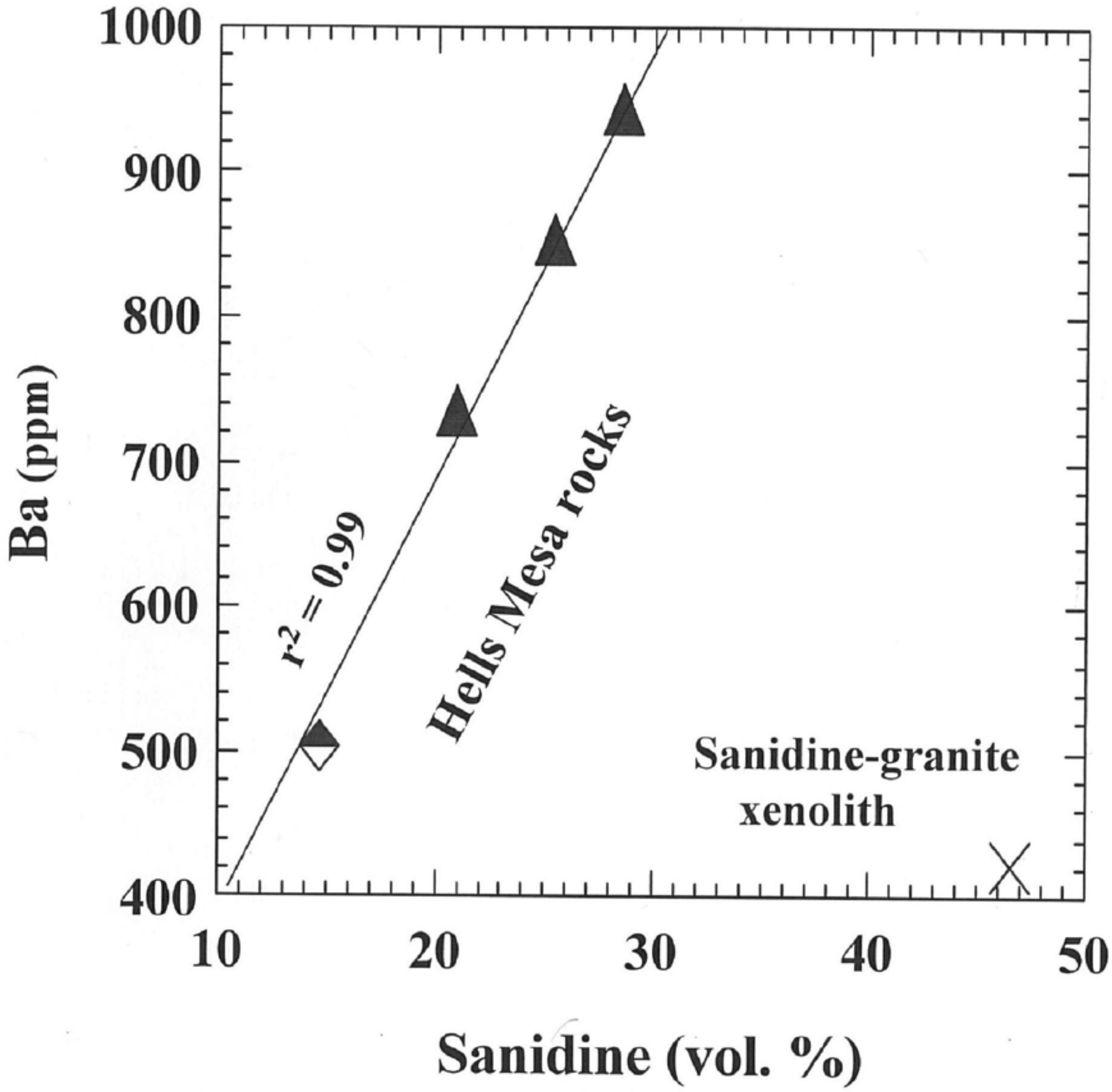

Figure 8. Barium (Ba) vs. sanidine content for unaltered Hells Mesa rocks near the Esperanza mine and a sanidine-granite xenolith in dome-derived tuff breccia (Trt). Symbols are as shown on Figure 7. Data from Tables 1 and 2; samples E1, E2, E3, E6, and E4.

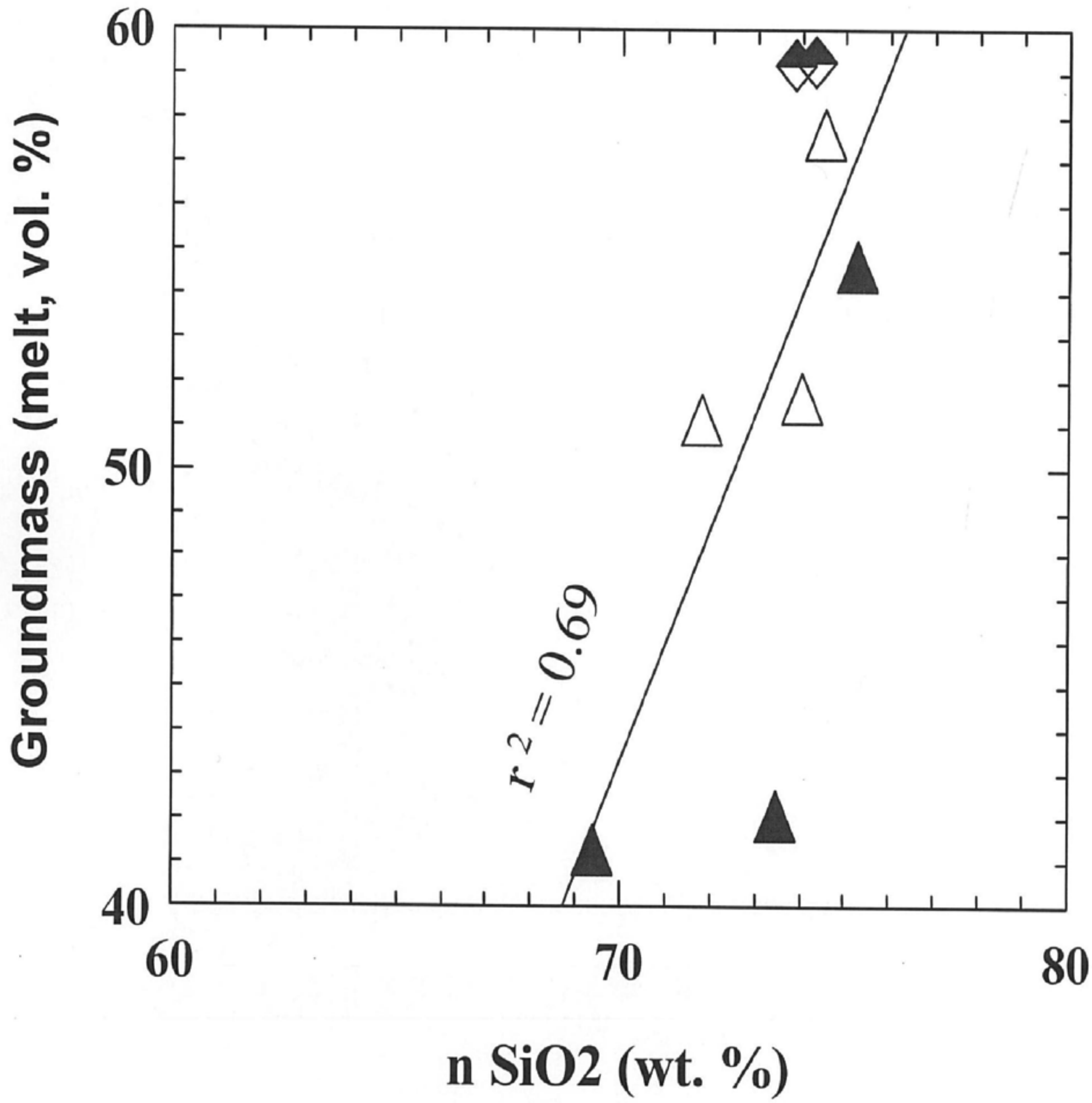

Figure 9. Normalized SiO_2 vs. groundmass (melt) content in caldera-facies Hells Mesa Tuff and comagmatic lava-dome rocks. Symbols are as shown on Figure 7. Data from tables 1and 2; samples E1, E2, E3, E6, and B1-B4.

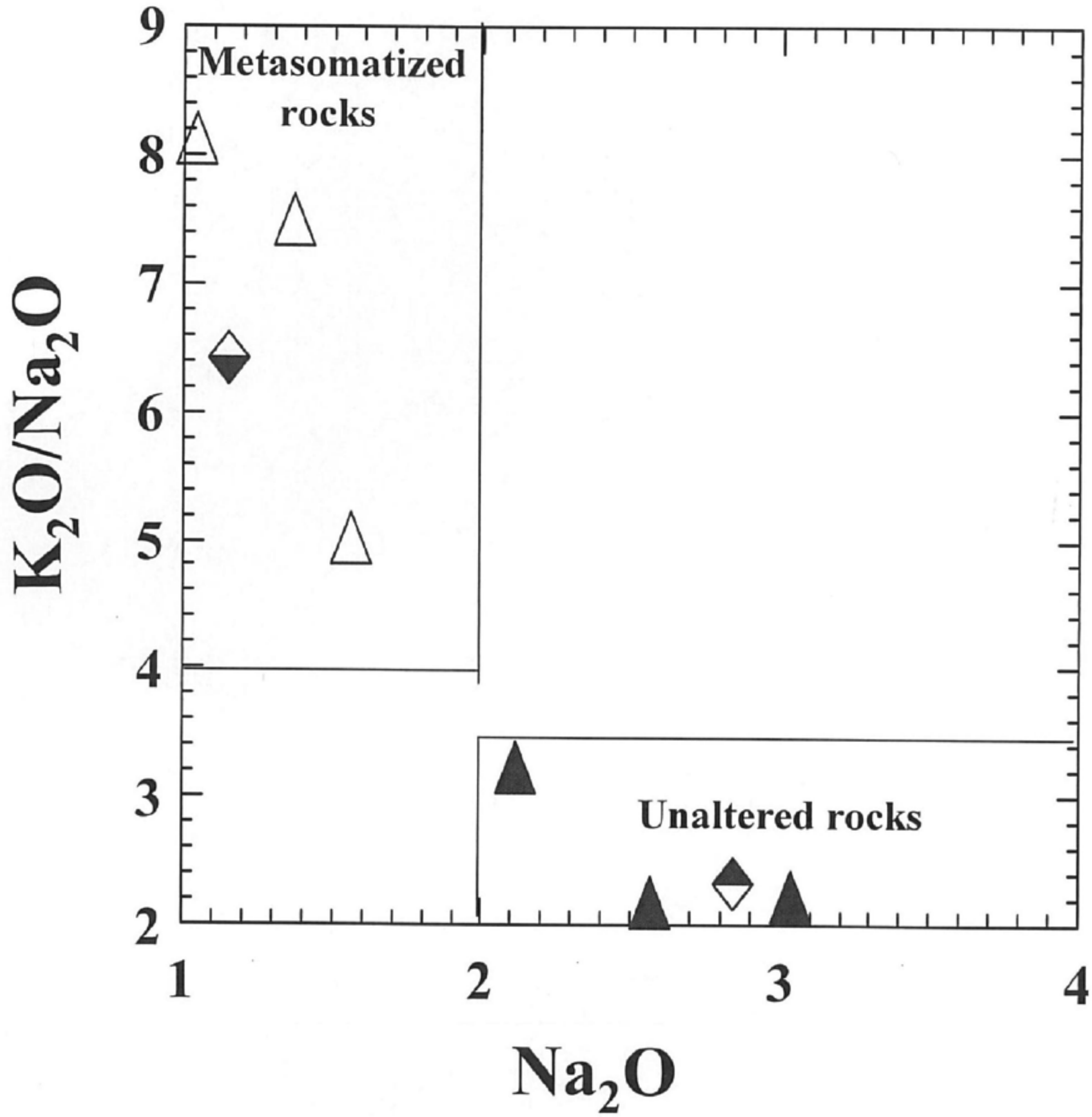

Figure 10. K_2O/Na_2O vs. Na_2O for K-metasomatized Hells Mesa rocks near the Bursum mine and unaltered Hells Mesa rocks near the Esperanza mine. Symbols as shown on Figure 7. Data from Table 2; samples E1, E2, E3, E6, and B1-B4.

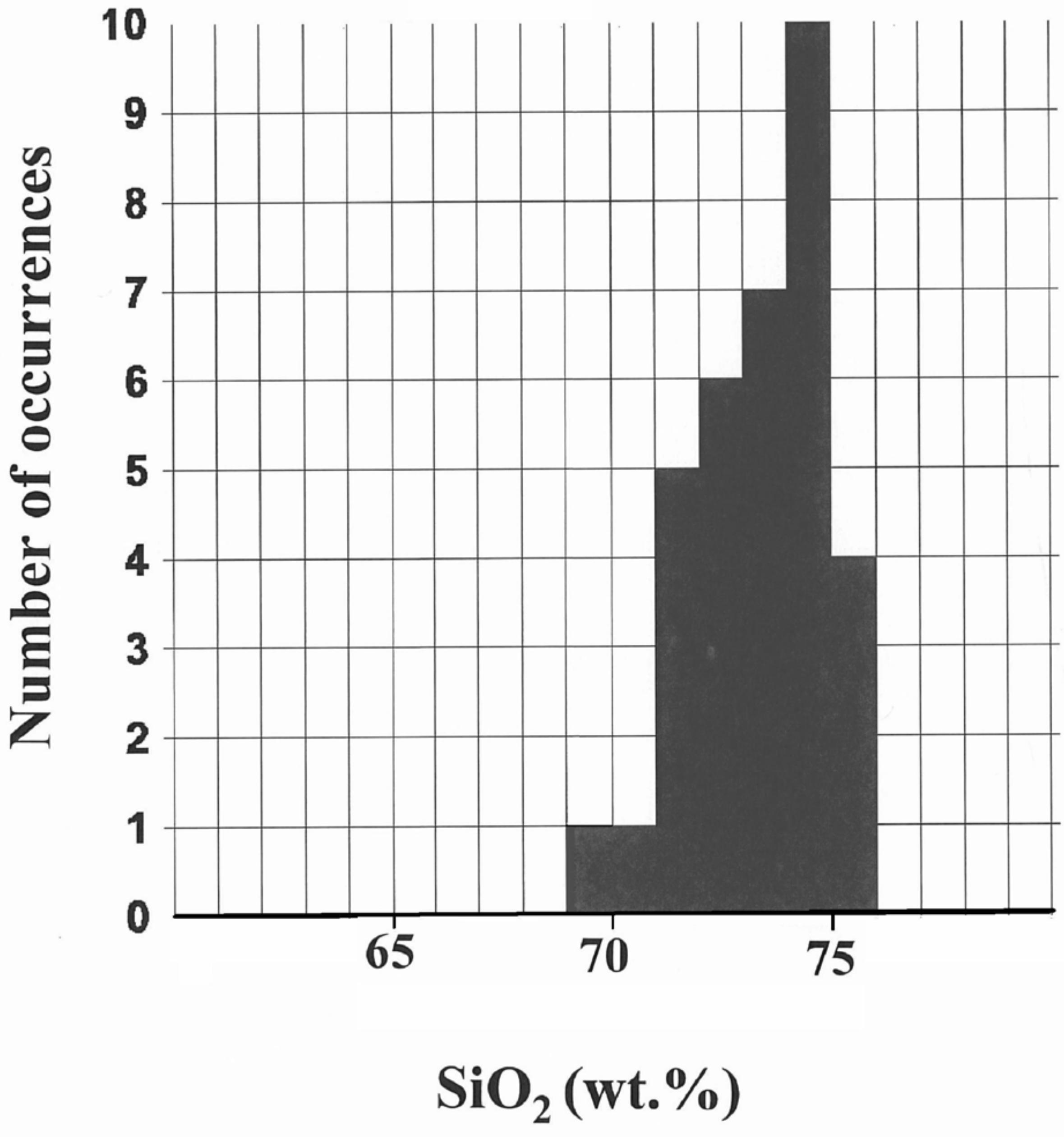

Figure 11. Histogram showing SiO_2 variation in the Hells Mesa eruptive suite (n=34). Normalized select data from Table 5.

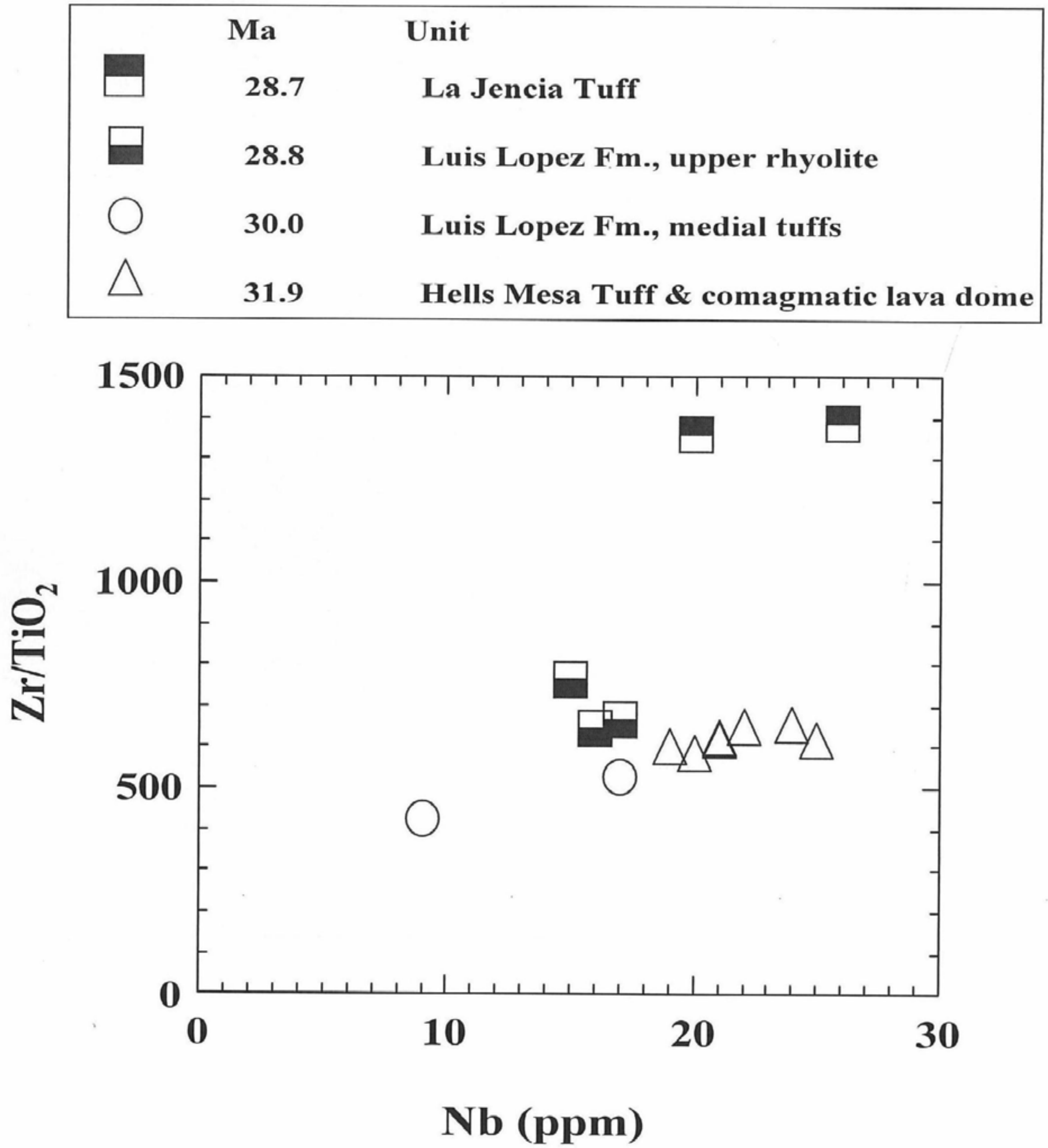

Figure 12. Zr/TiO_2 vs. Nb for Oligocene rhyolites erupted from the eastern Socorro caldera. Data from Tables 2 and 8.

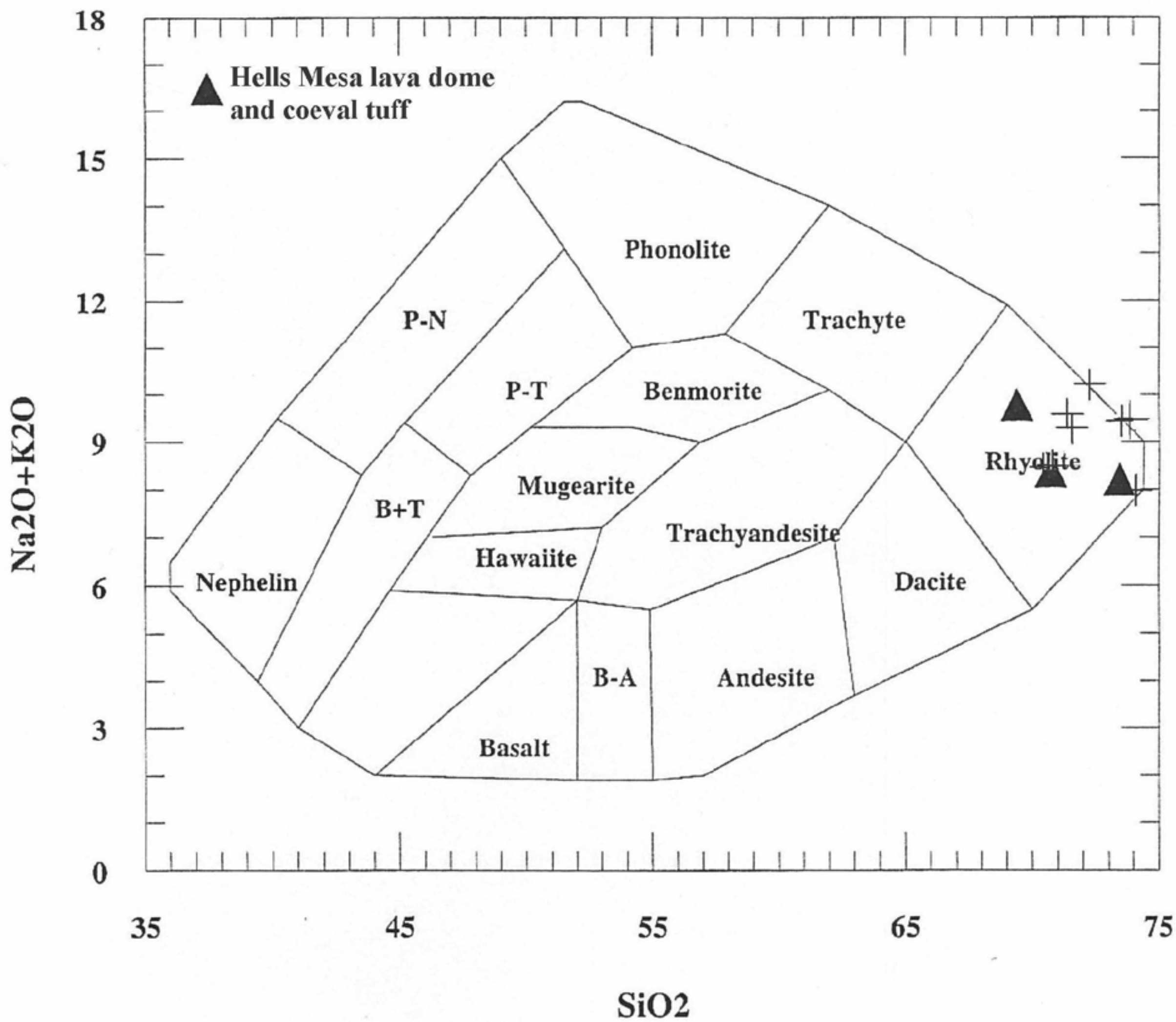

Figure 13. Total alkali-silica classification of unaltered Hells Mesa rocks (Cox, 1979). Data from Table 7.

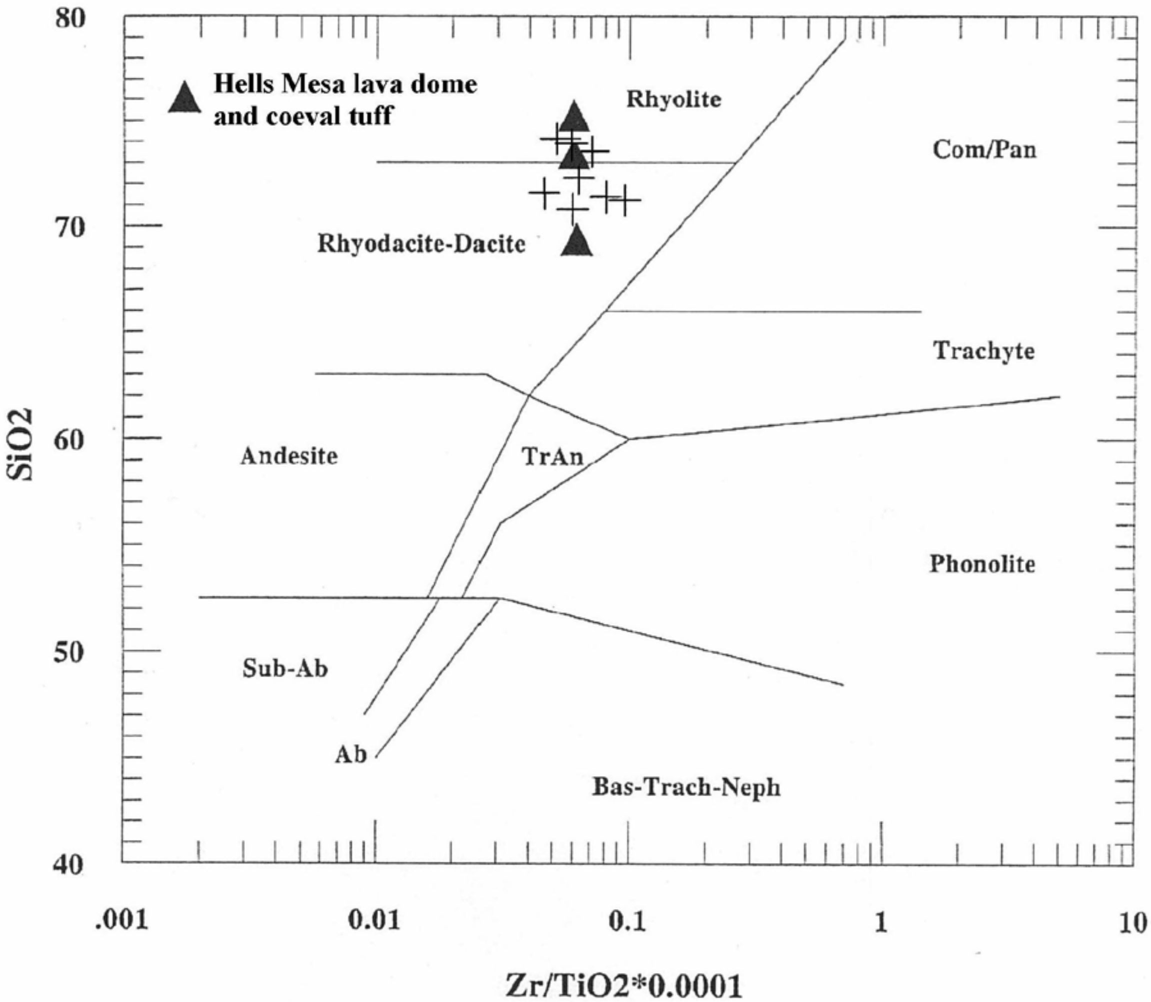

Figure14. Immobile element discrimination diagram (SiO2 vs. Zr/TiO2) for unaltered Hells Mesa rocks (Winchester and Floyd, 1977). Data from Table 7.

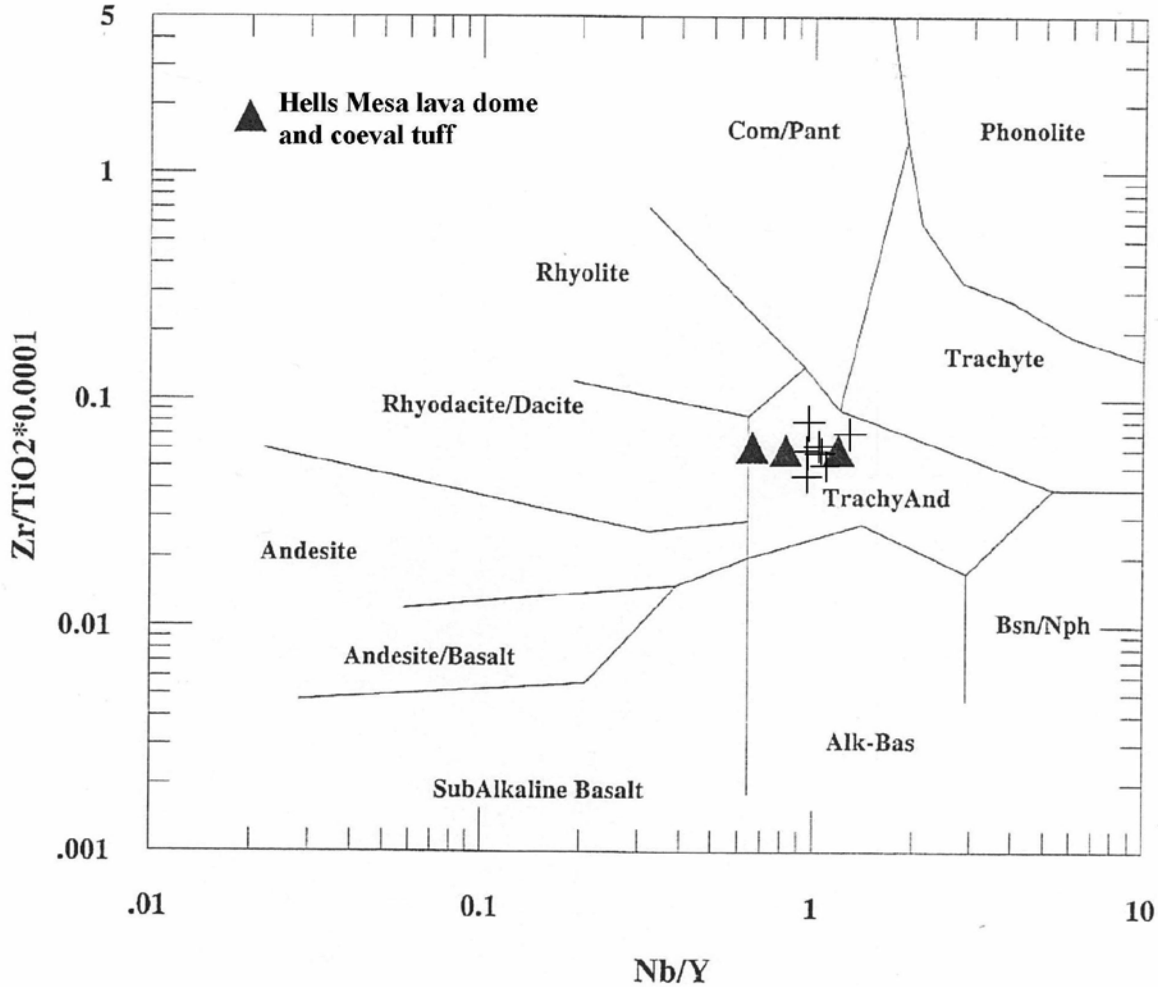

Figure 15. Immobile element discrimination diagram (Zr/TiO_2 vs. Nb/Y) for unaltered Hells Mesa rocks (Winchester and Floyd, 1977). Data from Table 7.